CORNELL UNIVERSITY

DESIGN BUILD FLY

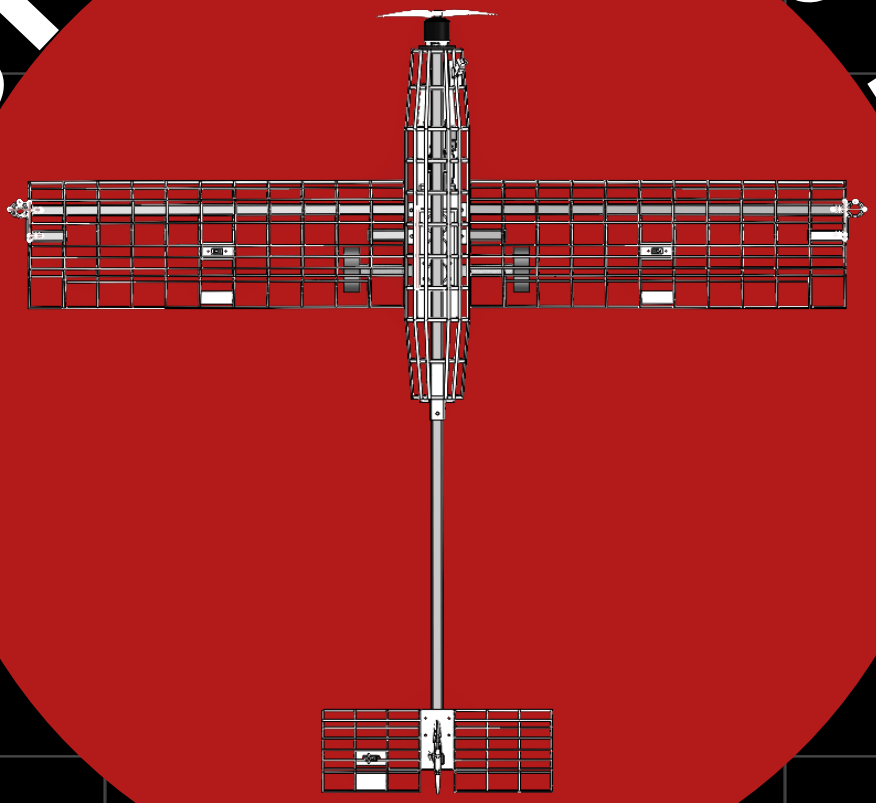

2022-2023

DESIGN REPORT

AIAA, TEXTRON, RAYTHEON

Contents

1 Executive Summary

The following document serves as the Cornell University Design Build Fly team's design report for the 2022-2023 AIAA Design Build Fly competition, detailing the team's structure, design, analysis, fabrication, and testing of a remote-controlled battery-powered aircraft designed to carry out electronic warfare missions.

The aircraft is required to be capable of performing three flight missions as well as a ground mission. Mission one serves as a staging flight with no payload demonstrating stable sustained flight. Mission two serves as a surveillance flight loaded with an electronics package payload. Mission three serves as a signal-jamming flight with a jamming antenna mounted on one of the wingtips. The ground mission serves as a structural integrity test, with the aircraft suspended on the wingtips and test weights applied to the center of the aircraft. The total score is a function of the mission scores as well as the design report score.

CU DBF utilizes a highly iterative approach to conduct and finalize its design for its entry in the 2022-2023 competition. This begins with a detailed reading of the rules, where scoring analysis and sizing analysis take place. At the same time, trade studies are conducted to define the optimal configuration. Following this, CAD models are generated and the team begins fabrication of the first iteration. Once testing of the first iteration was concluded, the team noted certain areas of improvement within subsystems and revisited the CAD before undertaking a second iteration of the aircraft. This process repeats until a highly optimized aircraft is fabricated and high performance is demonstrated.

BR-23 Vermillion's design consists of a tapered fuselage with hatches for easy installation of the electronics package, a modular low-wing with dihedral, a conventional tail, and a single tractor propulsion system to provide ample thrust. BR-23 is designed to be modular with easily interchangeable subsystems to allow for quick assembly on the flight line. Additionally, the wings and fuselage are equipped with two carbon-fiber spars to provide structural support for the aircraft. These spars are crucial as they sustain the majority of lift and weight forces and must be robust. A notched box makes up the mission two electronics package which is housed in the fuselage. Additionally, the six-inch jamming antenna for mission three attaches to the wing through a resin 3D-printed adapter that also interfaces with the ground test fixture, also fabricated in-house. The team estimates missions one and three to be complete in 2.91 minutes and ten sustained laps for mission two carrying a 2.65-pound electronics package, with the mission three antenna length set at six inches.

The remainder of this design report provides 1) an overview of the team and team structure, outlining the team organization, workflow, and timeline, 2) a discussion of the conceptual design process including the mission requirements, a scoring sensitivity analysis, and trade studies to determine the overall configuration, 3) the preliminary design process detailing the design and analysis methodology, how sizing was conducted, and aerodynamic analysis, 4) the detailed design of BR-23's subsystems, key parameters, flight performance estimates, and a CAD drawing package, and 5) a description of how manufacturing and various tests were completed, as well as results from those tests.

2 Management Summary

The Cornell University Design Build Fly team is made up of 29 undergraduate students. All members collaborate with each other in their respective subteams, each having their respective responsibilities.

2.1 Team Organization

Team leadership consists of two full team leads and a vice lead/safety officer. The full team leads are primarily responsible for the technical direction of the team, guiding design decisions and aircraft development, and for logistical aspects of the team's operations, including directing recruitment, onboarding of new members, and managing scheduling. The vice lead/safety officer ensures safe manufacturing operations and provides advice toward design decisions while assisting the team leads in operating the team. Additionally, a faculty advisor provides technical insight and feedback during design and report reviews.

Furthermore, the team is organized into four teams as depicted in Figure 2.1.1: three technical subteams and one business subteam. The four subteams, distinguished by responsibility and function, consists of 25 technical members involved in aircraft design as part of the Aerodynamics and Controls, Mechanical Structures, and Propulsion subteams, and four members as part of the Business subteam. Each subteam has two subteam leads, who are responsible for directing subteam level activities, ensuring relevant subsystem requirements are met, and interfacing with the team leads. The specific role of each subteam, and the individual skill sets required of members in each are presented in Table 2.1.1.

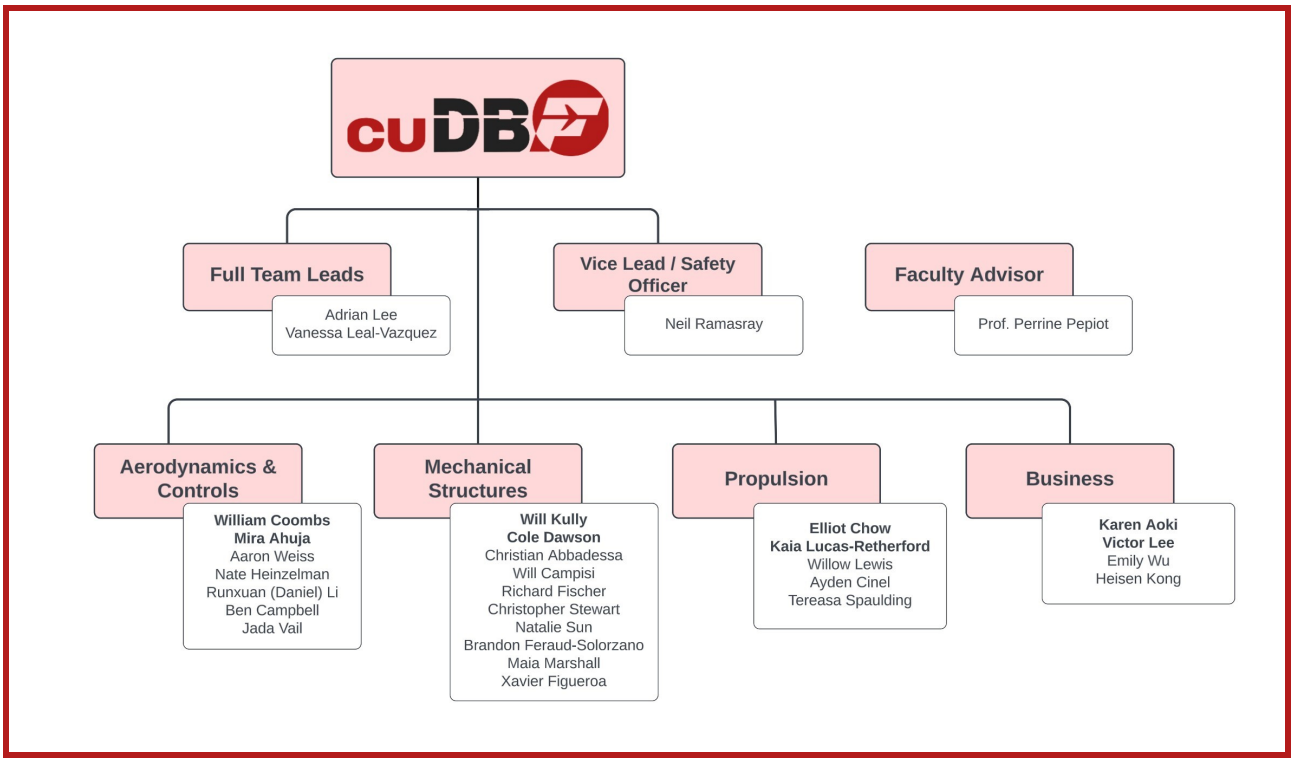

Figure 2.1.1: CU DBF's organizational structure. Subteam leads are bolded.

2.2 Operational Cadence and Communication Flow

The team's typical weekly operational cadence is depicted in Table 2.2.1. Most design tasks are initially delegated as general responsibilities to the subteam leads. It is then their role to distill the implied individual tasks, assign those to subteam members, and track that progress to ensure the broader responsibility is fulfilled. Meetings typically serve to get everyone on the same page, with more direct communication generally being conducted through Slack along with announcements made to the team or subteams.

Subteam	Responsibilities	Individual Skillsets
Aerodynamics and Controls	Responsible for flight performance, conducting sizing and scoring analyses. Designs and integrates the following subsystems: Wing, Empennage, Control Surfaces	Comprehensive knowledge of aerodynamic theory, proficiency in SOLIDWORKS and MATLAB, specialization in XFLR5, XFoil, and other aerodynamics analysis tools
Propulsion	Responsible for configuration selection, development, and integration of the following subsystems: Propulsion, Avionics	Comprehensive knowledge of motor, battery, and propeller selection using ECalc; proficiency in soldering and wiring with components including receivers, ESCs, servos
Mechanical Structures	Responsible for mechanisms and structures of the aircraft. Designs and integrates the following subsystems: Fuselage, Landing Gear, Mission-Specific Mechanisms	Comprehensive knowledge of statics and mechanics of materials, proficiency in SolidWorks, MATLAB, and/or ANSYS
Business	Directs team marketing and outreach, manages team budget and purchases	Strong organizational and communication skills, familiarity with web design and social media

Table 2.1.1: Subteam Responsibilities and Skillsets

2.3 Timeline and Milestones

The team's planned and actual development timeline, along with major milestones, can be found in Figure 2.3.1.

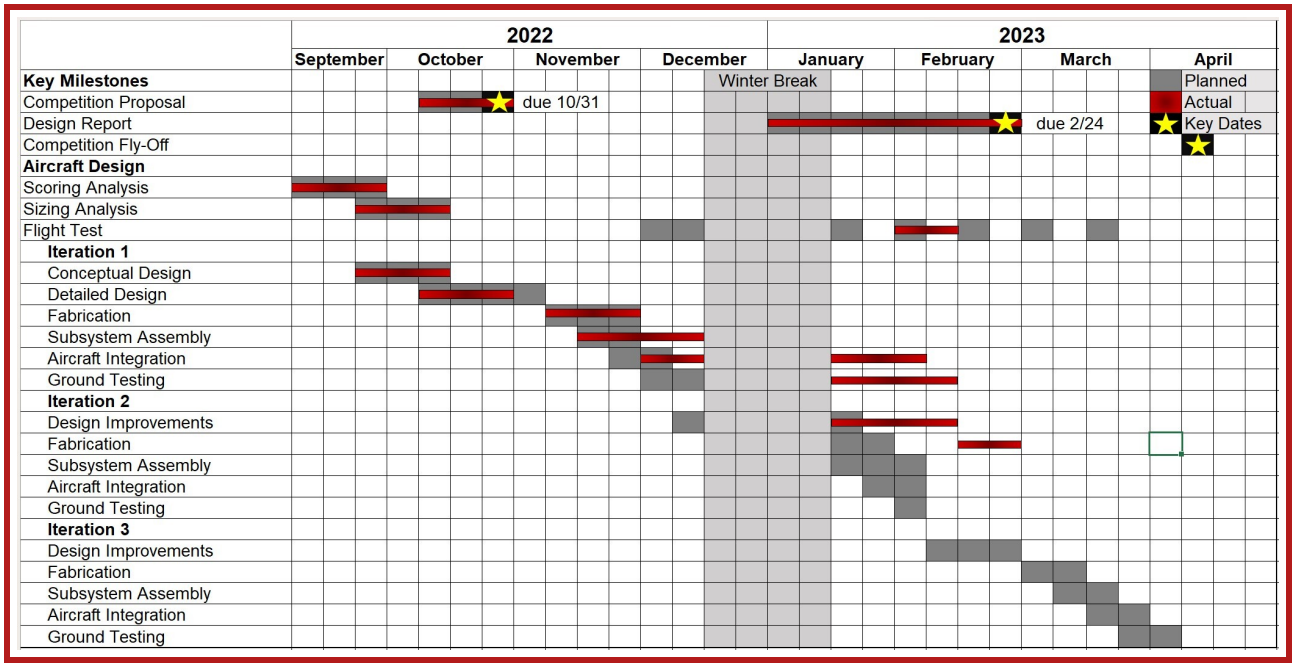

Figure 2.3.1: Gantt Chart of Planned and Actual Development Timeline

Day Of The Week	Event/Meeting	Purpose
Monday	All-Hands Meeting	Reflect on successes and challenges of past week; Ensure unified understanding of tasks and goals for upcoming week; Maintain broad overview of current team status and timeline
Tuesday	Leads Meeting	Ensure leads and subteam leads have a shared understanding of current progress on delegated responsibilities; Address any concerns and act on new challenges; Maintain active awareness of team morale and academic workloads
Wednesday-Friday	Subteam Meetings / Subteam Work Session	Facilitate shared understanding of subteam goals by all members; Delegate tasks and follow up on individual responsibilities; Progress checkpoint comparing to goals set during All-Hands Meeting
Saturday	All-Hands Work Session	Make progress on outstanding action items, with presence of all members facilitating communication and interaction between subteams/subsystems

Table 2.2.1: Weekly Operational Cadence

3 Conceptual Design Approach

3.1 Mission and Design Requirements

This section outlines the requirements and constraints for the four missions of the 2023 Design Build Fly Competition. In these missions, the requirements and specifications have been deconstructed and translated into a set of system requirements that subsystems must be capable of achieving. System requirements have traceability to the rules [1] while the subsystem requirements have traceability to the system requirement they fulfill, and all have a method of verification (V), either by inspection (I) or testing (T). These requirements served as a basis for configuration discussions among subteams and explore various design choices. Table 3.1.1 lists the requirements the aircraft must achieve.

In the scoring equations detailed in Sections 3.1.1, 3.1.3, and 3.1.4, the team's score (N) is normalized by the maximum mission score attained by the teams attending the fly-off (Max).

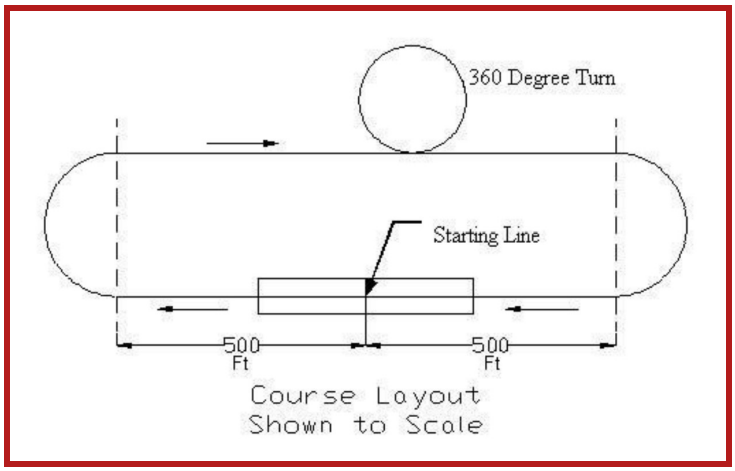

Figure 3.1.1: Flight Path for Each Lap

Req	#	Requirement Description	V	Traceability
SIZE	1	All components shall fit inside a box of 62 linear inches.	I	AIAA DBF Rules
SYS	1	The shipping box and all components shall weigh less than 50 pounds.	I	AIAA DBF Rules
	2	The aircraft shall hold the M_2 electronics package.	T	AIAA DBF Rules
	3	The aircraft shall hold the M_3 jamming antenna on either wingtip.	T	AIAA DBF Rules
	4	The aircraft shall take off within 60 feet of the start/finish line.	T	AIAA DBF Rules
	5	The aircraft shall complete three laps within a five-minute window.	T	AIAA DBF Rules
	6	The aircraft shall be assembled for flight within five minutes.	I	AIAA DBF Rules
	7	No component shall be released from the aircraft during flight.	I	AIAA DBF Rules
	8	The aircraft shall be unmanned.	I	AIAA DBF Rules
	9	The aircraft shall be flown in the same configuration for all three missions excluding the M_3 jamming antenna and counterweight.	I	AIAA DBF Rules
	10	The aircraft shall be flown by a human pilot with a remote-control system.	I	AIAA DBF Rules
PROP	1	The aircraft shall sustain flight for at least 10 minutes.	T	SYS 5
	2	Brushed or brushless electric motors shall be used.	I	SYS 4, 5
	3	The aircraft shall have one or more motors.	I	SYS 4, 5
	4	The motor mount shall withstand motor forces.	T	SYS 5, 7
AVIO	1	Any single propulsion system shall be powered by a maximum of one battery pack.	I	SYS 4-6
	2	The aircraft shall be fitted with a LiPo battery-operated propulsion system not exceeding 100Wh.	I	SYS 4-6
	3	All battery packs shall be identical.	I	SYS 6
	4	The battery positioning may differ between missions.	I	SYS 2
	5	The propulsion system shall be fitted with an arming plug and a blade-style fuse.	I	SYS 4, 5
MECH	1	The minimum weight of the electronics package shall be equal to or greater than 30% of the gross vehicle weight.	I	SYS 2, 6
	2	The electronics package shall have minimum dimensions of 3.00 x 3.00 x 6.00 inches.	I	SIZE 1, SYS 2
	3	A jamming antenna of ½ inch Schedule 40 PVC pipe shall be securely attached to one wing tip.	I	SYS 3
	4	The fuselage shall have a door or hatch for payload accessibility.	I	SYS 2
	5	The electronics package shall not extrude outside of the aircraft's external surfaces or features.	I	SYS 2
AERO	1	Two identical sets of the left and right wings shall be manufactured.	I	SYS 1-7
	2	The aircraft shall include a dihedral.	I	SYS 1-7
	3	The aircraft shall fly at takeoff gross weights of 4.29 lbs, 6.92 lbs, and 4.51 lbs for M_1, M_2, and M_3 respectively.	I	SYS 1-7
	4	All control surfaces shall deflect properly.	T	SYS 4-5

Table 3.1.1: Aircraft systems-level requirements

3.1.1 Ground Mission

This mission is a demonstration of the aircraft's structural margin where all the aircraft parts and payloads will start inside the shipping box. Upon flipping a coin twice to determine the wing set, the assembly crew member along with the pilot will have a 10-minute window to assemble the aircraft, install the payload, install the ground test fixture and apply the test weights. Particularly, the assembly crew member is responsible for assembling the airplane and installing the heaviest payload configuration as declared at technical inspection. Additionally, they will install the structural test fixture onto the wing tips and apply test weights to the center of the aircraft fuselage until the max weight is achieved or time expires, whichever is first. These weights must be applied inboard of the wing section attachment joint and any aid or adapter will be included in this weight. While in this configuration, the pilot is responsible for making sure the flight controls are working properly. Once the final test weight is applied, there will be a 30-second hold and at this time, the pilot will again verify that all flight functions are still nominal. If there is no structural failure or deformation, the final weight will be recorded on the score sheet; otherwise, the test has failed. Scoring for this mission is a function of the total test weight divided by the max aircraft weight, where the total test weight is the test weight that was applied plus the max aircraft weight.

$$GM = \frac{\text{N}_{\text{total test weight / max aircraft weight}}}{\text{Max}_{\text{total test weight/max aircraft weight}}} \tag{1}$$

3.1.2 Mission 1: Staging Flight

The aircraft must enter the staging box while still inside its shipping box, after which a coin will be flipped to determine the wing set used for the mission. The assembly crew member will then have five minutes to assemble the aircraft for flight. The aircraft's takeoff field length must be less than 60 feet, and it must successfully complete three laps around the designated flight course within a five-minute time window and land in order to get a score. A lap is deemed complete when the aircraft crosses over the start/finish line while in the air. Timing for Mission 1 starts when the throttle of the aircraft is advanced for its first takeoff attempt and ends after the completion of lap three. Landing is not part of the five-minute time window. The score for mission 1 is 1.0 for a successful mission.

$$M_1 = \begin{cases} 1.0 & \text{Successful deployment} \\ 0 & \text{Unsuccessful deployment} \end{cases} \tag{2}$$

3.1.3 Mission 2: Surveillance Flight

Mission 2 requires an electronics package payload with minimum dimensions of 3.00 x 3.00 x 6.00 inches and must be carried internally to the aircraft. No part of the electronic package can be part of or extrude outside of the airplane's external surfaces or features. The weight may be varied to achieve higher scores with a maximum weight declared at technical inspection. The maximum weight will be measured and recorded in pounds at technical inspection. The minimum weight of the electronics package must be equal to or greater than 30% of the gross vehicle weight flown during that mission. The aircraft must enter the staging box while still inside its shipping box, after which a coin will be flipped to determine the wing set used for the mission.

The assembly crew member will then have five minutes to assemble the aircraft for flight. The takeoff length must be less than 60 feet and there will be a 10-minute window for this mission. Timing starts when the throttle is advanced on the first takeoff attempt, and a lap is complete when the aircraft passes over the start/finish line in the air. The landing is not part of the 10-minute window, but a successful landing must be completed to obtain a score. Post-flight, the aircraft and electronics package will be weighed to verify that the payload weight is equal to or greater than 30% of the gross vehicle weight of the aircraft flown and to record the payload weight. The mission 2 score is then calculated as per Equation 3.

$$M_2 = 1 + \frac{\text{N}_{\text{payload weight} \times \text{laps flown}}}{\text{Max}_{\text{payload weight} \times \text{laps flown}}} \tag{3}$$

3.1.4 Mission 3: Jamming Flight

The payload for this mission is the jamming antenna, which must be attached to an aircraft wingtip while it completes three laps around the designated flight course. The aircraft must enter the staging box while still inside its shipping box, after which a coin will be flipped to determine the wing set that will be used for the mission. The jamming antenna must be mounted on the aircraft side opposite the flight safety line in the direction of takeoff. The takeoff length must be less than 60 feet and there will be a five-minute window to complete the mission. Time starts when the throttle is advanced on the first takeoff attempt. Time ends after the aircraft completes its third lap. A lap is completed when the aircraft crosses the start/finish line in the air. The aircraft must land in order for the mission to be scored, but landing is not included in the five-minute time limit. The Mission 3 score is then calculated as per Equation 4.

$$M_3 = 2 + \frac{\text{N}_{\text{antenna length/time}}}{\text{Max}_{\text{antenna length/time}}} \tag{4}$$

3.1.5 Overall Scoring

The team's score will be calculated using the competition report score, the total mission score, and a participation score. Participation (P) will be scored one point for attending the fly-off, two points for completing the technical inspection, and three points for attempting a flight mission. These scores will be computed using the following formulas:

$$\text{Total Mission Score} = M_1 + M_2 + M_3 + GM \tag{5}$$

$$\text{Total Score} = \text{Report Score} \times \text{Total Mission Score} + P \tag{6}$$

3.2 Sensitivity Study of Design Parameters

Following the release of the rules specifications, the Cornell team identified key parameters determining each mission's score, namely the Mission 2 package weight (and thus, speed) and Mission 3 antenna length. Additionally, the team needed to understand how varying different parameters would affect the total flight score attainable. Thus, the team developed a robust MATLAB[2] script that takes into account the mission scoring equations (equations 1- 4), key aerodynamic equations, and the overall feasibility of certain geometries.

Notably, Mission 1 and ground mission parameters were ignored due to the nature of the missions; Mission 1's score is based solely on whether the aircraft is deployable for flight, and the ground mission is based solely on the structural integrity of the aircraft, something not easily quantifiable at the conceptual design stage.

Of the two parameters selected for analysis, the package weight had a greater impact on the total mission score, as shown in Figure 3.2.1. The mission score is approximately four times as sensitive to the package weight compared to the antenna length. This indicates that the priority of this year's aircraft lies in maximizing the electronics package weight, although the effect of a longer antenna is also significant in the mission score.

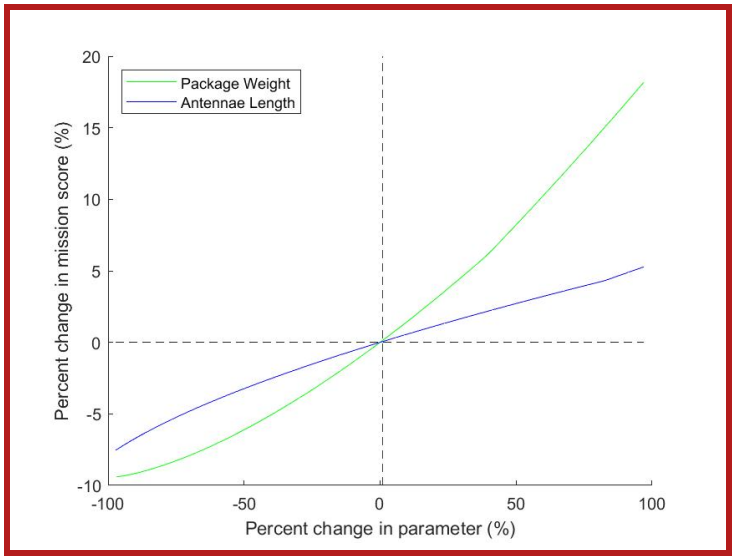

Figure 3.2.1: The results of the MATLAB sensitivity analysis of mission score to the electronics package weight and antenna length.

Another observation not accounted for numerically is the effect of a fast aircraft. Both Missions 2 and 3 have a time element involved, with the number of laps flown in ten minutes directly correlated to the cruise speed of the aircraft. A high cruise speed can be achieved by creating a light aircraft and a powerful propulsion system to maximize the lap speed. Taking both the numerical results from the sensitivity analysis and the importance of flight speed, the goal of the team shifted to finding the optimal weight where speed can be maximized while housing a heavy electronics package.

3.3 Configuration Selection and Trade Studies

The purpose of conceptual design and trade studies is to take the requirements set out in Table 3.1.1 and consider various aircraft designs, before determining the overall aircraft shape. This aircraft shape then drives the preliminary design process, allowing the team to produce numerical values for the different subsystems before the final design is complete. To do this, trade matrices are generated to numerically weigh different options based on various parameters, including, but not limited to, ease of manufacturing, aerodynamics, overall strength, and stability. The team is then able to select optimal configurations for the aircraft build.

3.3.1 Aerodynamics Trade Studies

Each configuration was chosen based on aerodynamic capabilities, advantages for completing competition missions, and manufacturability. The aerodynamics score represents how well a specific configuration generates lift, how stable it flies, and how well it handles maneuvers such as turns, takeoffs, and landings. The mission score represents how well a specific configuration would improve the team's ability to maximize mission scores, specifically: how well it would be able to fit in the shipping box (SIZE 1), how much lift it could generate when carrying a heavier electronics package (MECH 1-2)(AERO 3), and how the configuration would handle a long antenna (MECH 3). The manufacturing score represents how feasible it would be to design and manufacture, which is especially important given that two sets of wings must be manufactured. These considerations are quantified in trade matrices.

Aircraft Configuration The conventional aircraft configuration (distinct wing, tail, and fuselage) was chosen due to its reliability and large payload volume (MECH 2, 5). However, unique aircraft configurations such as the flying wing and flying V configurations were also taken into consideration.

The flying wing configuration allows for less drag and structural weight. It also reduces wing loading and requires a smaller wetted area. Additionally, this configuration enables a shorter takeoff roll. However, this is not a significant concern for this year's competition missions. More importantly, this configuration is unable to accommodate a large payload, complicated to design, and harder to control [3], so the flying wing configuration was rejected.

The flying V configuration would allow for a reduced wetted area, and therefore reduced friction drag. This configuration also requires less structural weight due to fewer bending moments from fuel and the payload. This configuration, however, would cause many problems during the manufacturing process because it includes both an inner and outer wing, and because the payload is laterally distributed in the flying V configuration. There is also a risk of inducing a strong pitching-up moment since the outboard wing stalls first, possibly requiring additional components such as a leading edge slat or droop nose[4]. Lastly, this configuration requires large landing gear legs due to the absence of trailing edge flaps [4]. For these reasons, the flying V configuration was rejected.

Despite the relatively larger structural weight and drag compared to the two configurations, the conventional aircraft configuration was adopted for this year's competition aircraft for its many advantages. The team is more familiar with designing and manufacturing such an aircraft and this allows for more resources and configuration choices while designing the wing, tail, and integration pieces. The necessary interior volume for keeping the Mission 2 payload is simpler to incorporate as well. For these reasons, a conventional aircraft configuration was determined to be the best option.

Options	Aerodynamic Score	Mission Score	Manufacturing Score	Total Score
Conventional Aircraft	**3**	**4**	**5**	**12**
Flying wing	4	2	2	8
Flying V	4	1	1	6

Table 3.3.1: Aircraft Configuration Trade Matrix

Wing Configuration The wing configuration choices considered were the wing height and wing geometry as well as the presence of dihedral, flaps, and taper. A rectangular low-wing with a dihedral, no flaps, and no taper was chosen based on mission requirements, ease of manufacturing, and aerodynamic characteristics.

A mid-wing configuration has good flight characteristics, being a compromise of low and high-wing configurations. However, mid-wing configurations require the wing spar to pierce the center of the fuselage, which reduces the storage capacity of the fuselage and prevents the electronics package from being placed close to the wing where it would have minimal effects on the center of gravity. Also, it would require adjustments to the fuselage to allow for adequate structural stability as its rib structure is weakest in the center, adding more unnecessary weight. For these reasons, a mid-wing design was rejected.

With only high and low wing configurations left, it was most efficient to compare the two directly. In terms of aerodynamics, a low wing has a lower drag profile, allowing for an increased cruise airspeed, which is important for Mission 2's longer flight time (PROP 1) and faster completions of Missions 1 and 3 (SYS 5). A high wing however has better roll stability as the center of gravity is below the wing while a low wing requires a dihedral to offset its instability (AERO 2), which increases the manufacturing and design complexity of the wing integration and the Mission 3 adapter. A high wing also provides better indications of an impending stall than a low wing, but the aircraft should be flying at higher speeds and at relatively low load factors, reducing the risk of stall. For the Mission 3 antenna, the high wing configuration induces a high pitching moment due to form drag as the antenna is far above the center of gravity while a low wing places it very close to the center of gravity, so it affects the flight characteristics less. A high wing makes landing and takeoff easier for the pilot, but this aspect is not especially significant as the maximum allowed takeoff distance is long, and only one takeoff and landing is performed per mission (MECH 6). In terms of assembly, both designs are very similar. A high-wing design would be easier to assemble as the plane would not have to be flipped over to attach the wings but the landing gear needs to be attached with the plane flipped (MECH 8). While a high wing has advantages, the low wing configuration was chosen as it has better characteristics for the missions and optimizes for higher mission scores.

Options	Aerodynamic Score	Mission Score	Manufacturing Score	Total Score
High Wing	5	3	5	13
Mid Wing	4	2	3	11
Low Wing	**4**	**5**	**4**	**13**

Table 3.3.2: Wing Configuration Trade Matrix

Wing Geometry For wing geometry, a rectangular non-tapered wing was chosen. Taper does provide slightly higher lift efficiency as opposed to the rectangular wing for a basic planform wing (97% to 94% lift efficiency for a basic planform aspect ratio, AR, seven wing) and may fit more easily in the shipping box (SIZE 1). However, it is more difficult to manufacture than rectangular wings using the laser-cutting process due to combs attaching to the ribs at non-perpendicular angles. This is an important consideration, given that two identical sets of wings needed to be built. Additionally, a tapered wing provides less area on the wingtip to attach to the Mission 3 adapter.

Special wing geometries were also considered but ultimately not used due mainly to their manufacturing

limitations. The sweptback geometry often creates a dangerous stall pattern mid-flight, and it is significantly harder to manufacture and integrate [5]. Also, this wing geometry is used primarily for transonic speeds, not applicable for a battery-powered remote-controlled aircraft.

An elliptical wing geometry was also considered for its uniform stall and 100% lift efficiency (for AR=7 and basic wing planform) due to the fact that the lift load across a wing usually forms in an elliptical distribution, minimizing the induced drag [6]. However, it is significantly harder to manufacture, especially with wood laser cuts and MonoKote procedures, encouraging an inherently rectangular design. An elliptical wing geometry is also not ideal for double-wing manufacturing and optimizing shipping box space because it would create gaps and waste volume. It also does not have an ideal placement for a mission 3 integration piece. Thus such a geometry would add a lot more complexity for minor benefits.

Options	Aerodynamic Score	Mission Score	Manufacturing Score	Total Score
Rectangular w/ taper	5	4	4	13
Rectangular w/o taper	**4**	**5**	**5**	**14**
Sweptback	3	3	1	7
Elliptical	5	1	2	8

Table 3.3.3: Wing Geometry Trade Matrix

Additional Wing Parameters During the preliminary design process, flaps were considered because they allow for short takeoffs and landings and are useful near stall speeds. However, the aircraft will be ideally flying at full speed for the duration of all missions. Adding flaps drastically decreases the aileron length, and the takeoff field length is long enough to not necessitate prioritizing large amounts of lift at low speeds. Thus, including flaps was less important (SYS 4) than elongating the ailerons to prioritize maneuvering capabilities.

Dihedral was added to the wing configuration because there was a concerning amount of roll instability in the preliminary XFLR5 analysis of the desired wing configuration with zero degrees of dihedral (see Section 4.4.2). While including dihedral complicates the manufacturing of the integration piece, dihedral significantly improves the aerodynamic handling characteristics and can eliminate roll instabilities. Additionally, as the team decided on a low-wing aircraft, which generally has more maneuverability at a cost of less stability, a dihedral became necessary to counteract some of these effects. Section 4.4.2 provides a more detailed commentary about the benefits of dihedral and how much to put.

Options	Aerodynamic Score	Mission Score	Manufacturing Score	Total Score
Without Dihedral	2	4	5	11
With Dihedral	**5**	**4**	**3**	**12**
Without Flaps	**5**	**5**	**5**	**15**
With Flaps	4	3	4	11

Table 3.3.4: Additional Wing Parameters Trade Matrix

Tail Configuration The tail configurations considered were the conventional, T-tail, H-tail, and V-tail. A conventional tail configuration was chosen based on its relatively low weight, ease of manufacturing, aerodynamic characteristics, and box geometry.

The main tail configuration where weight would be a significant concern is the H-tail due to a second vertical stabilizer. The V-tail would require less weight for the configuration itself but likely additional weight would be needed for both the V-tail and T-tail configurations to add structural integrity. This makes the conventional tail the most viable option in terms of weight.

For manufacturing, a tail configuration that was simpler to construct was preferred due to the amount of work that is needed to build the two sets of wings. The conventional tail was also used in the 2021-2022 competition entry, so the members were already familiar with the design and manufacturing of this configuration. The H-tail and V-tail would require more time and research effort as well as involve more potential areas for issues and structural stability. A V-tail would also likely be more difficult to construct (especially in letting the glue cure) due to its slanted surfaces.

In terms of aerodynamic considerations, an H-tail has a more efficient horizontal stabilizer but is a better configuration for a two-propeller plane, which was not what was used in this aircraft. A V-tail has reduced drag but would be more complex to pilot. The benefit of the T-tail over a conventional tail would be that the airflow over the chosen low-wing configuration would not disrupt the airflow over the tail because they would not be at the same height. This was resolved by using a high tail configuration in relation to the fuselage. A T-tail also provides greater control in spins but is susceptible to deep stalls, neither of which are anticipated maneuvers to be intentionally performed. Due to the limited advantages of other configurations, a conventional tail was still preferred.

In terms of the mission requirement of fitting in the box, there was very limited space for fitting the tail (see Section 4.2.5). A single vertical stabilizer was easier to fit in its limited dimensions as opposed to the double vertical stabilizer in an H-tail or slanted surfaces of the V-tail. A T-tail may have been slightly easier to fit in the box since the spar could be placed along the bottom, but the horizontal stabilizer of both the conventional tail and T-tail fit well in relation to the other parts.

Options	Aerodynamic Score	Mission Score	Manufacturing Score	Total Score
Conventional Tail	**4**	**5**	**5**	**14**
T-Tail	3	4	3	10
H-Tail	4	3	3	10
V-Tail	3	3	3	9

Table 3.3.5: Tail Configuration Trade Matrix

3.3.2 Mechanical Structures Trades

Fuselage Configuration The selection of the fuselage design is one of the most important decisions impacting the structure of the aircraft. The fuselage must be able to accommodate a sizable weighted payload for Mission 2 (MECH 1, MECH 5) while also withstanding the forces felt by the wings during Mission 3 (MECH 3) and ground tests. All of these factors must be considered while also allowing for the integration of the wing, tail, propulsion system, and electronic components required for flight. Table 3.3.6 depicts the trade matrix used to quantify configuration choices. Ultimately, a semi-monocoque fuselage consisting of balsa and basswood was selected.

A solid wall fuselage allows for the use of long sheets of wood instead of individual ribs. This contributes

to an overall greater mechanical strength of this design compared to others. Additionally, this method requires fewer pieces for construction, allowing for an easier manufacturing experience. However, some flaws posed large problems that needed to be addressed. One example of this is that the larger pieces of wood would make the plane heavier than other designs. Additionally, this design would be difficult to repair because of the size of each piece. If one part of the design were to fail, then it could require a whole new fuselage to be constructed.

Alternatively, a monocoque design uses ribs to form the main structure of the fuselage instead of solid walls. A thick covering is wrapped around these ribs to complete the body. This was the lightest of the proposed designs, requiring the least amount of wood. Despite this, the design had several key issues that led it to be unsuitable. The team has typically relied on MonoKote, a thick plastic, to form the outer structure of the plane. Due to the lack of internal support, this would be unusable as an external covering. Additionally, integrating this design with the wing, tail, landing gear, and Mission 2 mechanisms would be difficult given the overall low structural strength.

Lastly, the team considered a semi-monocoque design that uses ribs with connecting stringers to create the contours of the fuselage. This has a moderate weight and allows for greater mechanical strength than the monocoque design because of the stringer supports. Also, MonoKote can be used as a coating method without losing significant structural strength, allowing us to better size the overall dimensions of the fuselage (MECH 2). Another benefit of this design is that in the event of a crash, parts can be salvaged for other iterations. A possible drawback of this design is that a large number of pieces increases the manufacturing and assembly time.

Another aspect explored was the materials used for the construction of the fuselage. Traditionally, Cornell DBF uses a mixture of balsa and hardwood sheets: balsa for an overall lightweight fuselage, and hardwood to reinforce locations susceptible to elevated levels of mechanical stress. Alternatively, carbon fiber is a lightweight yet extremely strong material that can be used to construct the body of the aircraft.

A carbon fiber fuselage would have stronger mechanical properties than a wooden fuselage at a comparable weight. However, treating and utilizing carbon fiber for a fuselage is difficult for CU DBF. Cutting carbon fiber would require the use of a band saw or rotary cutting tool, and creating the structure would require a more involved layering process. Additionally, carbon fiber is much more expensive than the wooden alternative. In contrast, while the wood design may be structurally weaker, the team has access to wood-cutting machines, like laser cutters, that allow for components to be manufactured quickly and with little intervention. Wood sheets required for the fuselage parts are cost-effective and allow for multiple improvements and iterations.

Fiberglass was another option considered for the main structural material of the fuselage. Fiberglass has a notably significant resistance to bending and tensile/compressive stresses comparable to that of carbon fiber, while even being more cost-effective than carbon fiber. However, due to the team's lack of prior experience in fiberglass composites, implementation of fiberglass would require additional research and time to fully utilize its potential in structural applications.

Landing Gear Configuration Three landing gear configurations were considered as shown in Table 3.3.7: tricycle, taildragger, and tandem. The tandem gear was the most aerodynamic and stable thanks to the main wheels being placed in a line along the fuselage, with smaller wheels being placed on the wings for increased

Parameter	Options	Cost Score	Manufacturability Score	Mechanical Strength Score	Total Score
Fuselage Overall Design	Solid Wall	2	3	5	10
	Monocoque	5	3	1	9
	Semi-Monocoque	**4**	**4**	**4**	**12**
Fuselage Material Choice	**Balsa**	**5**	**5**	**3**	**13**
	Carbon Fiber	1	1	5	7
	Fiberglass	2	2	4	8

Table 3.3.6: Fuselage Trade Matrix

stability. However, due to the stress the extra wheels would have placed on the wings, as well as the difficulty of integrating them (AERO 1), the tandem gear did not score very well in the end. The taildragger configuration would have made for a generally solid gear and been useful for a short takeoff length, but the biggest concern was how it would integrate with the rest of the aircraft. The aircraft would be placed at an incline, making it difficult to keep the payload for Mission 2 and the batteries steady, as well as complicating the process of loading the aircraft during the ground mission and Mission 2. Ultimately, the tricycle configuration proved to be the most optimal and was selected. It keeps the plane level to the ground while scoring relatively high in every scoring category, creating a durable and stable gear.

Parameter	Options	Aerodynamic Score	Manufacturing And Integration Score	Structural Integrity Score	Stability Score	Takeoff And Landing Score	Total Score
Landing Gear	**Tricycle**	**4**	**4**	**5**	**5**	**5**	**23**
	Taildragger	3	3	4	3	4	17
	Tandem	5	1	2	5	2	15

Table 3.3.7: Landing Gear Trade Matrix

Mission 2 Payload Design Ensuring a secure attachment to the aircraft is one of the most important parts of the mission's success since an insecure weight could shift in flight and lead to a crash. Another major parameter that was discussed was the dimensions, but it quickly became apparent that the best solution would be to set the dimensions of the payload to the minimum dimensions allowed by the competition to limit the internal fuselage space the package takes up, allowing it to be moved to adjust the position of the center of mass of the aircraft.

The first method discussed for securing the payload was using notches in the box to fit into holes in the baseplate. This idea is simple to make and easy to insert, however, even small tolerance issues could lead to the loading moving in flight. Furthermore, the restriction that the notches would provide would likely not be strong enough to withstand the entire mission, so a stronger solution would be necessary.

Another concept for securing the box in the plane was to screw the payload into either the baseplate or the spar. This idea appeared much more viable than notches since screws would significantly limit the payload's ability to move in flight. Despite this, the constraint on aircraft assembly time (SYS 6) means that this solution is not feasible, as installing screws would be difficult to accomplish during the time constraint.

The third concept discussed was to use strong Velcro. While the Velcro may not be as strong as screwing the payload in, it provides sufficient adhesion for the mission. It is also much quicker to install which reduces the chances of issues. Ultimately, the team decided to use Velcro to secure the payload and additionally include two notches on the bottom of the payload to help ensure the package is held stationary during flight.

Paramter	Options	Strength Score	Manufacturing And Integration Score	Total Score
Attachment Method	**Velcro**	**4**	**5**	**9**
	Screwed-in	5	2	7
	Notched	2	5	7

Table 3.3.8: M2 Attachment Trade Matrix

Mission 3 Antenna Adapter The most important considerations for Mission 3 were the attachments between the PVC pipe and the adapter and between the adapter and the aircraft (MECH 3). If the PVC pipe and adapter are not well-fastened to the aircraft, the pipe could fall and detach or wobble, causing the team to fail the mission or have unstable aerodynamics. To ensure a well-fastened antenna, it was decided that precise manufacturing of the adapter, along with screws to apply pressure to the pipe, would ensure that it would not move during any phase of flight.

There were two basic designs proposed for the Mission 3 Integration Piece. The one which was eventually chosen was a small design with only the parts necessary to support a pipe and attach to the wingtip. The team also considered a version of the piece that would extend to the edges of the wing to form a streamlined shape to reduce drag. However, it was quickly decided that this would add a significant amount of weight and complexity for only minor aerodynamic benefits (AERO 3). Attempts to replace most of the resin in such a piece with a lighter material only partially eased these concerns, while increasing the complexity to a level that threatened to endanger the ease of assembly crucial to this year's competition. With these issues in mind, the team opted to simply minimize the volume, and thus the mass, of the final design, leading to a small, durable, and secure integration piece for Mission 3.

3.3.3 Propulsion Trade Studies

For the propulsion configuration, the tractor motor emerged as the best design choice from all the configurations considered (PROP 3). It is more aerodynamically stable and lightweight compared to the twin wing-mounted configuration. Additionally, a twin wing-mounted configuration would bring significant additional weight (as four wing halves must be manufactured) as well as take away time to assemble the aircraft to properly connect the motor wires. The tractor motor is also more efficient and easier to mount than both other designs considered. Ultimately, the pusher propeller was incompatible with the tail design, rendering it the

Parameter	Options	Strength/ Stability	Manufacturing	Mass	Integration	Total Score
M_3 **Integration Adapter**	**Aerodynamic**	**5**	**4**	**1**	**3**	**13**
	Minimal Volume	3	5	5	5	18
	Minimal Volume + Aerodynamic Shell	5	3	3	2	13

Table 3.3.9: Mission 3 Trade Matrix

most problematic configuration. Thus the tractor motor was chosen as the propulsion system of the aircraft.

Parameter	Options	Stability	Efficiency	Manufacturing & Integration	Total Score
Propulsion Configuration	Pusher Propeller	5	2	1	8
	Tractor Propeller	**5**	**4**	**5**	**14**
	Twin-Wing Mounted	2	2	3	7

Table 3.3.10: Propulsion System Trade Matrix

4 Preliminary Design

4.1 Design and Analysis Methodology

The team utilizes an iterative design and analysis approach that closely mirrors the systems engineering approach used by aerospace industry professionals. The development process, including all aspects of the design, build, and flight phases, is depicted in Figure 4.1.1.

A thorough and detailed reading of the competition rules set out in September allowed all team members to understand the mission requirements, leading to the development of sub-system requirements. These requirements provided a list of quantitative and qualitative items that needed to be fulfilled either through design or through ground or flight testing, as described in section 3.1. These subsystem requirements are further distilled in a set of trade studies that analyze the viability of different aircraft configurations. The main objective of these trade studies is to define the overall aircraft geometry and what the aircraft should look like approximately before going into further detail about exact dimensions. Additionally, the team began developing a scoring sensitivity analysis MATLAB script to gain a better perspective of the different objectives and what should be optimized for this year's aircraft. A preliminary design review concluded the conceptual design phase.

The sub-system requirements and results of the scoring sensitivity script allowed the team to progress

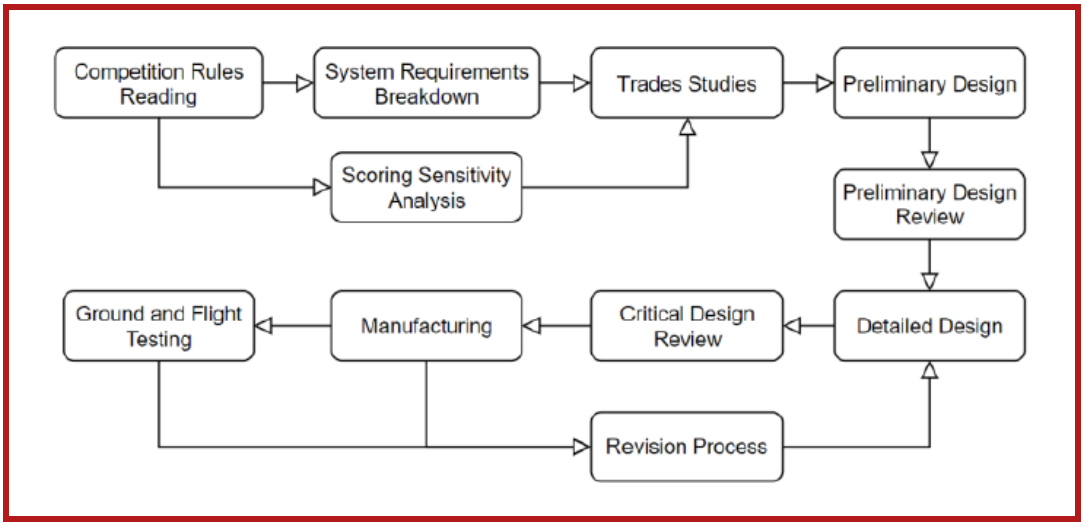

Figure 4.1.1: Team Design and Analysis Methodology

to the preliminary design phase. Notably, a separate sizing MATLAB[2] script, aerodynamic analysis utilizing XFLR5, and propulsion simulations using eCalc[7], were generated to determine quantitative benchmarks and design dimensions the aircraft needed to meet. These results helped refine the designs proposed in the conceptual design phase and develop subsystem and system computer-aided design (CAD) models. Subsystem and system critical design reviews allowed for team members and alumni to provide input and feedback before concluding the preliminary design phase and transitioning to fabrication and manufacturing.

Feedback from subsystem tests and flight testing allows the team to identify critical areas of improvement and propose solutions for future iterations. This allows an iterative design and analysis process where future iterations and prototypes improve on prior designs and lead to increased efficiency and higher-scoring flight scores.

4.2 Aircraft Sizing Procedure

From the results of the scoring sensitivity section (Section 3.2), the team decided to optimize for the Mission 2 score by designing an aircraft that can withhold a heavy load and fly efficiently. The shipping box and wing modularity presented a unique challenge to the dimensionalization of the aircraft. To optimize our aircraft under these constraints, the team developed a MATLAB script and used it with SOLIDWORKS to make sure all components could be housed in an airline-compliant box, be assembled quickly, and produce high mission scores.

4.2.1 MATLAB Sizing Script

One of the first design decisions the aerodynamics subteam made was to determine the aspect ratio of the aircraft. Aircraft typically have an aspect ratio between 6 to 8 [8]. Empirical data collected by observing planes from previous competitions shows that most RC planes built for those competitions operate well in this range. However, one of the challenges stipulated by the rules forcing a modular design necessitated a smaller aspect ratio. Thus the aerodynamics subteam opted for a reasonable aspect ratio of 6.

Additionally, the scoring sensitivity analysis highlighted the importance of maximizing the weight of the electronics package while maintaining a low takeoff weight to maximize the Mission 2 score (3). Starting with a reasonable initial Mission 2 package weight of 2.65 pounds, by the requirement that when loaded the package must be at least 30% of the total weight, a maximum takeoff weight of 8.81 pounds was estimated. This was a reasonable estimation, as CU DBF's aircraft from previous years requiring similarly sized payloads had a reasonably similar maximum takeoff weight.

With an initial maximum takeoff weight estimated, the team could now calculate the required surface area required of the wings. Wing cubic loading (WCL) serves as an accurate measure for grouping remote-controlled aircraft based on their flight characteristics and from an R/C perspective, acts as a better indicator than standard wing loading seen in traditional aircraft design [9]. Setting the WCL to 14, the upper limit of advanced sport RC aircraft, we can use Equation 7 to estimate the planform area.

$$WCL = \frac{MTOW}{(\frac{S}{144 \text{ sq ft/sq in}})^{1.5}} \rightarrow S = 144 \left(\frac{MTOW}{WCL}\right)^{\frac{1}{1.5}} \tag{7}$$

Equations 8 and 9 then estimate the wing geometry. The taper ratio was set to one; a decrease in the taper ratio significantly complicates the rapid fabrication of the wings as multiple wings need to be made for the modularity of the aircraft (AERO 1).

$$b = \sqrt{S \times AR} \tag{8}$$

$$c = \frac{b}{AR} \tag{9}$$

At this point, the geometric wing parameters are calculated and the team can proceed to size other subsystems.

4.2.2 Empennage Sizing

The empennage is designed to provide static and dynamic stability and control for the pilot to climb, descend, and yaw. The tail was sized using volume ratios as described by Daniel Raymer. Approximating our aircraft as a general aviation single-engine aircraft, we are able to use equations as well as tail volume coefficients as described by Table 4.2.1.

Type of Aircraft	Horizontal V_H	Vertical V_v
Sailplane	0.50	0.02
Homebuilt	0.50	0.04
General aviation - single-engine	0.70	0.04
General aviation - twin-engine	0.80	0.07
Agricultural	0.50	0.04
Twin turboprop	0.90	0.08
Flying boat	0.70	0.06
Jet trainer	0.70	0.06
Jet fighter	0.40	0.07
Military cargo/bomber	1.00	0.08
Jet transport	1.00	0.09

Table 4.2.1: Volume Ratios for Various Types of Aircraft [6]

$$V_H = \frac{S_H l_H}{S_w \bar{c}} \tag{10}$$

$$V_V = \frac{S_V l_V}{S_w b_W} \tag{11}$$

A challenge the team faced was sizing the tail arm as the tail spar could only be as long as the shipping box. The tail also was difficult to fit in as the horizontal and vertical stabilizers often exceeded the width and height of the shipping box during our tests. The team thus adjusted the aspect ratios and tail arm to allow the tail to fit. Vertical stabilizers typically have aspect ratios between 1.3 and 2, and the aspect ratio of the horizontal stabilizer should be less than that of the wing [10]. While taking the SA of the stabilizer calculated by having the largest tail arm that would fit in the box, the team optimized the AR of each in this range.

4.2.3 Fuselage Sizing

The minimum dimensions of the fuselage were constrained by the size of internal payloads and structural concerns. The fuselage needed to be large enough to hold the Mission 2 package along with the electronic components of the propulsion system. In order to hold the 3.00 inch by 3.00 inch package, the fuselage needs to include an internal cargo space area of 3.5 inches by 3.125 inches as a factor of safety. This led to a larger outer dimension of 5 inches by 6 inches in order to provide sufficient structural support surrounding the package, as well as space for wing and tail integration.

The maximum dimensions of the fuselage were constrained by the shipping box requirement. A longer fuselage provides more room to adjust the position of Mission 2 and tune the center of gravity of the aircraft for stability purposes. It also needed to be small enough to fit in the shipping box with other components. The team started with an overall fuselage length of 30 inches, a parametric measurement corresponding to half of the initially sized 60-inch wingspan. This was incrementally shortened as the size of the shipping box was finalized. Additional considerations were made for the motor and tail mechanisms. The team found that these components could not be installed correctly during the assembly time requirement and needed to be pre-attached to the fuselage. This drives a total fuselage length of 27 inches, with a 15 inch untapered cargo section to hold the Mission 2 package and some propulsion system electronics. The remaining length is divided between two 6 inch tapered sections at the front and rear of the fuselage to reduce flow separation while also avoiding steep slopes that would be challenging to manufacture and prevent easy storage of electronic parts.

4.2.4 Propulsion Sizing

To size the propulsion system of the aircraft, important values like minimum static thrust and thrust-to-weight ratio from sizing were used, as well as competition guidelines like flight time and maximum capacity to guide motor, battery, and propeller size selection. eCalc, a trusted R/C propulsion simulation, was the main software utilized to refine the propulsion system selection. Inputting variables given from the MATLAB sizing script (see Table 4.2.2) and varying one propulsion component at a time (battery, motor, propeller), various propulsion systems were analyzed and optimized to find the most efficient system.

In order to first determine the best motor for the system, the above values from the sizing script were fixed, as well as the propeller at a diameter of 12 inches and a pitch of 8 inches, an approximation that allows

Initial Sizing Parameters	Value (Units)
MTOW	8.81 lbs
Wingspan	63.5 in
Wing Area	672.04 in^2
Minimum T-W Ratio	0.486
Flight Time	11 minutes

Table 4.2.2: Sizing Parameters Inputted Into eCalc

us to choose other components. The battery was also fixed as a LiPo 4500mAh with 40C rating in order to maximize the capacitance (as shown in Table 4.2.4) according to the competition guidelines. Multiple motor combinations across different manufacturers and different Kv ratings were tested to try to optimize for the sizing parameters.

Once some viable options had been identified, they were narrowed down based on the objective dependent variables being tested for. Optimizing for the variables shown above, the list was narrowed even more. Table 4.2.3 denotes a few capable motors that satisfy the sizing requirements.

Motor	Flight Time (Mins)	Power (W)	Thrust/Weight Ratio	Mass (lb)
4-Max PPPO-5605-410 (410)	11.8	534	0.66	0.948
Aeolian C5055-KV400 (400)	11.7	582	0.69	0.606
Aeolian C5055-KV410 (410)	11.0	637	0.73	0.827
Cobra C-4120/22 (430)	11.5	555	0.68	0.646

Table 4.2.3: Capable motors satisfying requirements

The above table shows some of the important values recorded with each combination. Finally, market research was conducted to analyze which motors were realistically available for purchase at the price point. The Cobra C-4120/22 with a Kv rating of 430 was selected because it fit squarely within the parameters and is a trusted brand that could reliably be ordered from. Other options were either unavailable for purchase or sold out.

Using this set motor and battery, the propeller size and pitch were adjusted. With the selected battery and motor, a propeller diameter of 12 inches and pitch of 7 inches gave the best performance.

Battery Sizing In order to choose the best battery, multiple cell numbers were considered. Since the maximum energy from a single battery is limited to 100Wh (AVIO 2), several variations of cell number and voltage per cell were available for consideration. In order to maximize energy, only configurations that had about 100Wh of energy were considered. Table 4.2.4 reflects the different configurations explored. The chosen configuration was a 4500mAh battery with 6 cells connected in series, with each cell storing 3.7V. While an 8S configuration offered a greater voltage, the selected configuration was deemed the best configuration because it maximized nominal capacity.

Additionally, different manufacturers were considered when choosing the optimal battery. Table 4.2.5 lists a few considered manufacturers.

C-rating is defined as the amount of charge that can be safely discharged by the battery. The maximum continuous current can then be calculated as the product of C-rating and battery capacity. Using this relation,

Configuration	Maximum Total Energy	Nominal Voltage Per Cell	Number Of Cells	Nominal Voltage	Nominal Capacity
Configuration 1	100Wh	3.7V	6S	22.2V	4500mAh
Configuration 2	100Wh	3.7V	8S	29.6V	3380mAh

Table 4.2.4: Potential battery configurations

Battery Name	C-Rating	Weight (lbs)	Price	Dimensions
PULSE	40	1.66	$118.99	6.42in x 1.77in x 1.77in
Pyrodrone	120	1.52	$119.99	6.22in x 1.89in x 1.61in
Admiral	40	1.44	$89.99	6.38in x 1.81in x 1.61in

Table 4.2.5: Potential battery suppliers explored when choosing the optimal battery

the LiPo battery produced by Admiral proved to be the best option for its price and weight. The maximum continuous current is 180A given 4.5Ah and 40C.

This does not mean that the motor will be pulling at 180A. During normal flight, 100% throttle is rarely used except during takeoff and cruise throttle will be around 60-70%. Moreover, the current draw is not a linear relationship, so the team can expect a lower current draw when running the aircraft at cruise conditions.

In practice, the maximum current is never achieved as it is limited by the electronic speed control size, so the Admiral battery continues to be the optimal choice. The benefits of being lighter and cheaper made it an overall better choice (AERO 3). Therefore, out of these three batteries, the one produced by Admiral was chosen.

4.2.5 SOLIDWORKS Models

This year's competition cycle presents a unique challenge in that the wings must be interchangeable and able to be stored in an airline-compliant shipping box. Since the exact length, width, and height of the shipping box are left to each team to decide, the Cornell team used a script to optimize these dimensions as they directly relate to the dimensions of the aircraft. Initially, key aircraft dimensions were related to the shipping box geometry. However, it was difficult to visualize how shipping box dimensions relate to the aircraft's dimensions and how different aircraft configurations would affect arranging them.

To make sizing the plane and shipping boxes easier simple models were created in SOLIDWORKS. Models allowed for immediate feedback on how each iteration would look and the feasibility of such values. The models were made using variables so they could be adjusted simultaneously to match our script. The models are purposely bulkier than the sizes of the wings and other aircraft components. This was to account for a factor of safety from the predicted values to realized components. The shipping box was modeled as a frame so that the parts of the aircraft were observable and so that it was easy to visualize where the aircraft's body crossed the box's boundaries. These models helped in the experimentation of different ways to orientate the aircraft's components. Figure 4.2.1 shows the total proposed storage system that houses all of the aircraft components.

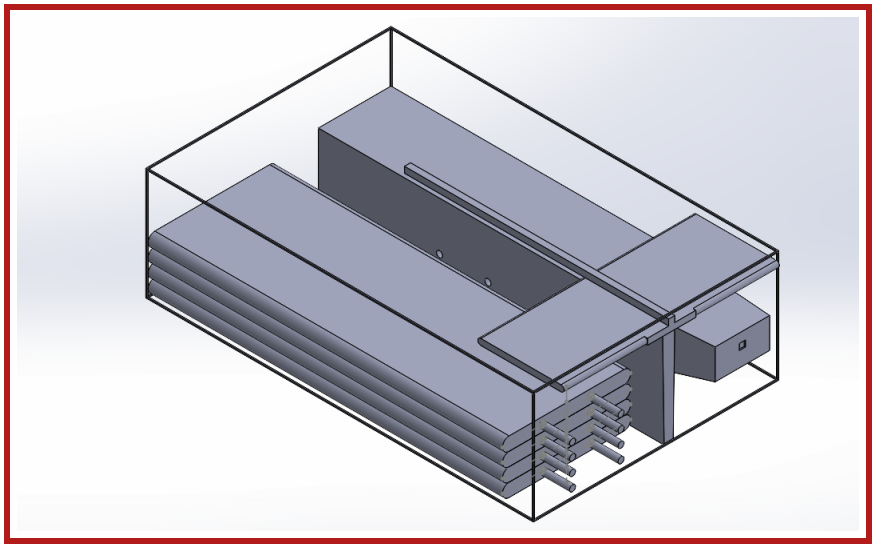

Figure 4.2.1: SOLIDWORKS Model of Preliminary Design Components Disassembled in a Compliant Shipping Box

Stacking the wings horizontally was the most efficient way to store them. The models made it clear what tail configurations were most volume efficient. The team determined that an H tail and similar configurations would take up too much volume for the desired stabilizer spans and chords. The shipping box model also showed that our finalized design fits inside the shipping box.

4.3 Airfoil Selection

This year, the CU DBF team considered the Clark V, MH114, NACA4412, SD7032, SD7062, and the USA-35B airfoils. These are all high-achieving airfoils that exhibit excellent lift and drag characteristics and have performed well in previous competitions and reports. The airfoil analysis was conducted in XFLR5, an aerodynamic analysis tool specializing in aerodynamic flows at low Reynold's numbers utilizing the vortex lattice method. According to the analysis in Figure 4.3.1, the MH 114 airfoil has the best lift and drag characteristics, though its camber concavity would pose a difficulty in manufacturing. Additionally, the SD7062 airfoil is the thickest of this set of airfoils, which would cause higher drag, shown by the Cl/Cd vs. Alpha graph between -10° and 10°. Contrarily, the SD7032 airfoil is the thinnest of this set, which would pose a threat of fragility. There were no manufacturing concerns with the Clark V, though it does not generate as much lift compared to the other airfoils. Both the NACA 4412 and USA-35B airfoils are easier to manufacture compared to higher performing airfoils, and this analysis shows that USA-35B performs better than NACA 4412; thus, CU DBF selected the USA-35B airfoil for the final design. Figure 4.3.2 depicts the general cross-section of the USA-35B airfoil.

4.4 Stability Analysis

4.4.1 Static Stability

Table 4.4.1 below contains data for the aircraft CG in the three missions. The masses of individual components were estimated, then the positions of those components were computed using the full CAD model (see Section

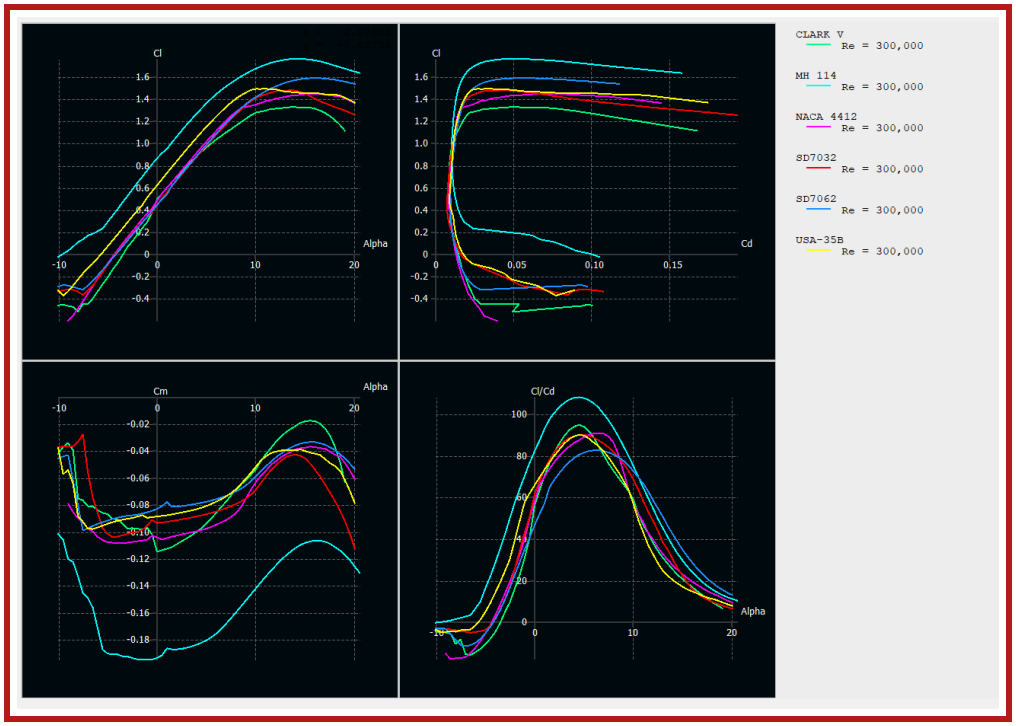

Figure 4.3.1: Clockwise From Top Left: Cl vs Alpha, Cl vs Cd, Cl/Cd vs Alpha, Cm vs Alpha for various airfoils

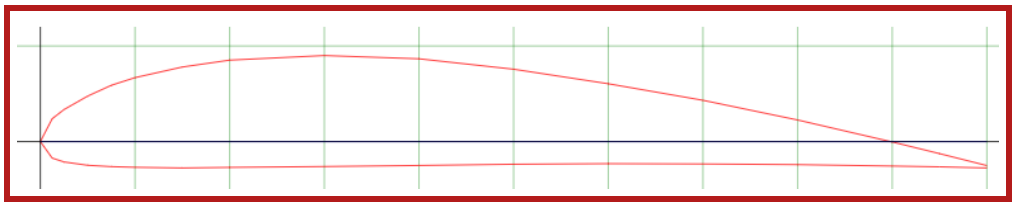

Figure 4.3.2: The USA-35B airfoil, chosen for XE-23

5.4). Each component was added as a point mass in XFLR5, and the total mass and the CG of the aircraft were calculated for the various flight missions. XFLR5 calculates the location of the center of mass using a coordinate system with the origin at the leading edge of the wing and on the aircraft plane of symmetry. The positive x-axis points aft along the fuselage, the positive y-axis points along the starboard wing, and the positive z-axis points upwards. The masses used in the initial analysis are a moderate underestimate, with various unaccounted components such as glue, MonoKote, and servos adding approximately 0.2 lbs to the final mass. However, this additional mass is distributed over the whole aircraft, and as such is not expected to substantially impact the CG.

Missions	m (lbs)	CG_x (in)	CG_y (in)	CG_z (in)
M_1	4.286	3.57	0.00	2.38
M_2	6.921	3.57	0.00	2.38
M_3	4.506	3.57	0.00	2.38

Table 4.4.1: Estimated Masses and Center of Gravity for various mission profiles

Using the values from Table 4.4.1, the static margin (SM) can be calculated. Static margin is a measure of an aircraft's longitudinal stability; the larger the static margin, the more longitudinally stable the aircraft is.

A static margin cannot be too large, however, because the larger the static margin, the more drag will be produced. Typical stable aircraft have a static margin ranging from 5% to 20% [8], so the team's target static margin for all three missions was set at 15%. Using a chord length of 9.92 inches set from sizing, the center of gravity in the longitudinal direction given by Table 4.4.1, and Equation 12, the team calculated the static margin for all three flight missions. Table 4.4.2 lists the outputs of these calculations. For each mission, the static margin remains at approximately 16%, thus validating the estimated center of gravity and ensuring a statically stable aircraft.

$$\text{SM} = \frac{\text{Neutral Point} - \text{Longitudinal Center of Gravity}}{\text{Mean Aerodynamic Chord}} \tag{12}$$

Flight Mission	SM (%)
M_1	0.156
M_2	0.160
M_3	0.164

Table 4.4.2: Calculated Static Margin for Various Mission Profiles

4.4.2 Dynamic Stability

A digital model of the aircraft was generated in XFLR5 to analyze its dynamic stability using a mix of the vortex-lattice method and the 3D panel method. Figure 4.4.1a shows the root-locus plot for the longitudinal modes for the three missions. Each longitudinal eigenvalue has a negative real component and a non-zero imaginary component, indicating that these modes are oscillatory and damped. Figure 4.4.1b shows the root-locus plot for the lateral stability modes for the three flight missions. As shown in the plot, the roll subsidence and dutch roll modes both have negative real components of their eigenvalues. This indicates that these modes are damped, and, as such, the roll and yaw oscillations will decrease with time, providing stability. The differences in eigenvalues between the missions for a particular mode are relatively small, except for roll subsidence, as shown by the dot clusters in the root-locus plots. This indicates that the aircraft design is not overly sensitive to mass distributions, providing a margin of error in construction. Tables 4.4.3 and 4.4.4 below summarize important values relating to the aerodynamic modes. All eigenvalues, natural frequencies, damping ratios, and time constants are within established acceptable ranges, indicating an airworthy aircraft.

The analysis in XFLR5 makes several assumptions, such as neglecting side slip, disregarding the skin friction drag due to the fuselage, and incomplete interactions between the fuselage and the wing; flight tests are required to determine whether or not the aircraft is truly airworthy or not and to validate the numerical results.

4.5 Lift and Drag Predictions

Table 4.5.1 contains predicted aerodynamic performance values for the aircraft. This analysis was conducted in XFLR5 using geometries and masses based on the finalized CAD assembly. The constructed mass of the aircraft is a bit higher, however, this additional mass is not believed to substantially impact the values below. Figure 4.5.1 below shows several graphs of the aerodynamic performance of the aircraft. Notably, the relations

Longitudinal modes	Natural frequency (F) (hz)	Damped Natural Frequency (F1)	Damping ratio (zeta)	Eigenvalue (lambda)
Mission 1 Short-Period Mode	1.60	0.98	0.89	$-7.91 \pm 6.17i$
Mission 1 Phugoid Mode	0.11	0.11	0.03	$-0.02 \pm 0.67i$
Mission 2 Short-Period Mode	1.74	1.15	0.75	$-8.23 \pm 7.24i$
Mission 2 Phugoid Mode	0.10	0.10	0.03	$-0.02 \pm 0.62i$
Mission 3 Short-Period Mode	1.67	1.06	0.77	$-8.14 \pm 6.65i$
Mission 3 Phugoid Mode	0.10	0.10	0.03	$-0.02 \pm 0.66i$

Table 4.4.3: Longitudinal Stability Modes for All Mission Profiles

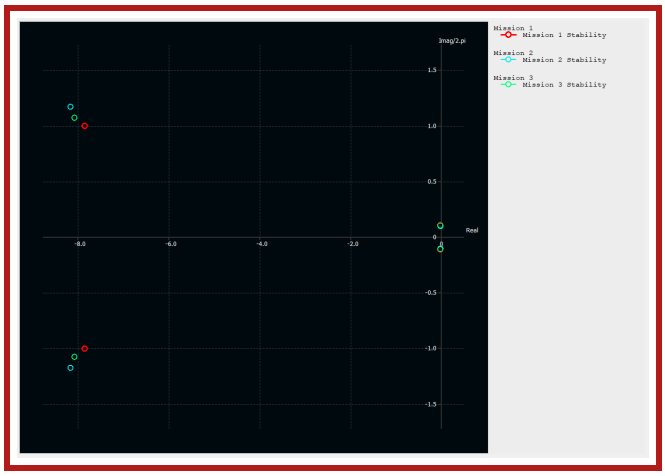

(a) Root-locus plot of longitudinal stability of all three mission profiles

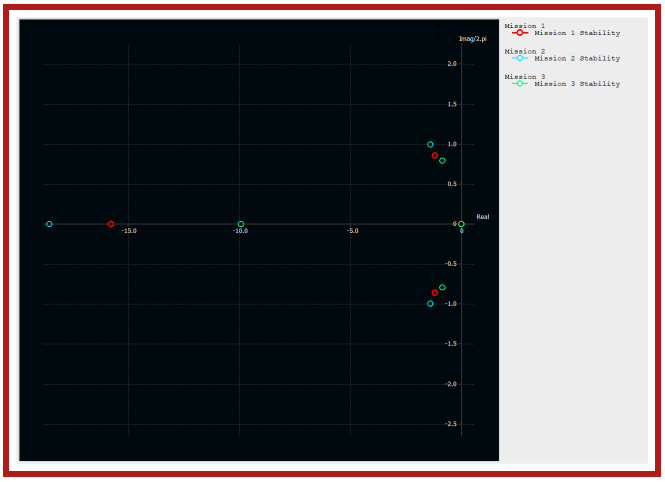

(b) Root-locus plot of lateral stability of all three mission profiles

Figure 4.4.1: Stability root locus plots for all flight modes and missions. The red, blue, and green dots indicate mission one, mission two, and mission three stability modes respectively.

between the quantities for the three missions are all approximately the same, which indicates that the aircraft will fly well for each mission.

4.6 Estimated Performance

The team's MATLAB script (outlined in Section 4.2.1 also takes the aircraft parameters to estimate the aircraft's cruise performance. The aircraft's Mission 1 estimated cruise speed is 42.65 ft/s while traveling with an angle of attack of 0.5 degrees. Using the competition rules diagram an estimated lap is on average 3000 ft. This gives an estimated lap time of about 70 seconds. Our aircraft is expected to perform Missions 1 and 3 in a little under 3.5 minutes and the aircraft should complete at least ten laps for Mission 2 if flown at cruise speed. Table 4.6.1 details the expected scores of each flight mission.

Lateral modes	Natural frequency (F) (hz)	Damped Natural Frequency (F1)	Damping ratio (zeta)	Time Constant (tau) (s)	Time to double(s)	Eigenvalue (lambda)
Mission 1 Roll Subsidence Mode	-	-	-	0.04	0.06	-15.77
Mission 1 Dutch Roll Mode	0.88	0.86	0.22	-	-	$-1.20 \pm 5.38i$
Mission 1 Spiral Divergence Mode	-	-	-	122.23	85.41	-0.01
Mission 2 Roll Subsidence Mode	-	-	-	0.05	0.04	-18.54
Mission 2 Dutch Roll Mode	1.02	1.00	0.22	-	-	$-1.40 \pm 6.24i$
Mission 2 Spiral Divergence Mode	-	-	-	97.49	67.57	-0.01
Mission 3 Roll Subsidence Mode	-	-	-	0.10	0.07	-9.87
Mission 3 Dutch Roll Mode	0.80	0.79	0.17	-	-	$-0.86 \pm 4.98i$
Mission 3 Spiral Divergence Mode	-	-	-	90.07	62.43	-0.01

Table 4.4.4: Lateral stability modes for all mission profiles

5 Detailed Design

The following section describes in detail the finalized design of BR23-Vermillion from a subsystem level, a center of gravity analysis, aircraft performance, mission performance, and a CAD drawing package.

5.1 Subsystem Design

5.1.1 Wing Detailed Design

Each half-wing is made up of 12 wooden ribs. The ribs at the root, tip, and center of the wing are made of hardwood as they experience the greatest forces. The remaining ribs are made of balsa as they will experience less force and thus can be made of less dense material saving weight. Figure 5.1.1 depicts a SOLIDWORKS rendering of the individual rib design.

With a taper ratio of 1 (a rectangular wing), the rib sizes are constant throughout. The thickness of the ribs, stringers, and plates are all $1/8$". This thickness was chosen as it provides a balance between structural

Variable	Meaning (units)	Performance, empty (M_1)	Performance, MTOW (M_2)	Performance, antenna (M_3)
m	Mass (lbs)	4.70	7.35	4.92
$C_{L,cruise}$	Coefficient of lift under cruise conditions	0.56	0.56	0.56
$C_{D,cruise}$	Coefficient of drag under cruise conditions	0.03	0.03	0.03
L/D_{cruise}	Lift-to-Drag ratio under cruise conditions	18.67	18.67	18.67
V_c	Cruise speed (ft/s)	42.65	53.34	44.00

Table 4.5.1: Expected Aerodynamic Performance for Each Mission

Variable	Meaning	Value
t_{M1}	Mission 1 Completion Time	3.52 min
v_{M2}	Mission 2 Estimated Speed	53.34 ft/s
t_{M3}	Mission 3 Completion Time	3.41 min
-	Estimated M_2 Package Weight	2.645 lbs
-	Estimated M_3 Antenna Length	6 in

Table 4.6.1: Expected Preliminary Design Performance Predictions

stability and weight reduction. The ribs have holes in them to reduce their overall mass. The ribs are connected by two hardwood spars, one carbon fiber spar, and multiple balsa stringers. The hardwood spars and stringers allow the wing to maintain the shape of the airfoil when covered by MonoKote. MonoKote, a plastic heat-shrink covering, is used because of its lightweight and low skin friction drag. The main carbon fiber spar spans the wings, giving them good structural stability and acting as the integration point between the wing and fuselage as well as the wing and Mission 3 connector. There are secondary carbon fiber spars at the tip and root that span only one rib. The secondary spars have wood rails underneath them to support their weight and increase the area of adhesion, providing structural stability and preventing wing flexing. The Mission 3 adapter is screwed into the carbon fiber spars. The wing is attached to the fuselage with clevis pins via an integration piece in the fuselage which is angled upwards to give the wings seven degrees of dihedral. The aileron servos are installed on a plate in the middle of each wing and protrude out of the bottom of the wing as to have the least effect on airflow. The ailerons have plates glued into them via wood glue, which are used to attach the control horns. Table 5.1.1 provide relevant dimensions of the wing and the ailerons.

At this stage, the wing design is complete. The left wing is shown in Figure 5.1.2.

5.1.2 Tail Detailed Design

The final design of the empennage consists of a conventional tail configuration comprising of a horizontal and a vertical stabilizer. The initial dimensions of the empennage were determined during the sizing process. However, during design reviews it was determined that the elevator and rudder chords needed to be increased to improve pitch and yaw control. After further design changes, the tail's updated parameters are listed in Table 5.1.2.

The horizontal stabilizer consists of six hardwood ribs and two balsa ribs. The elevator contains two balsa

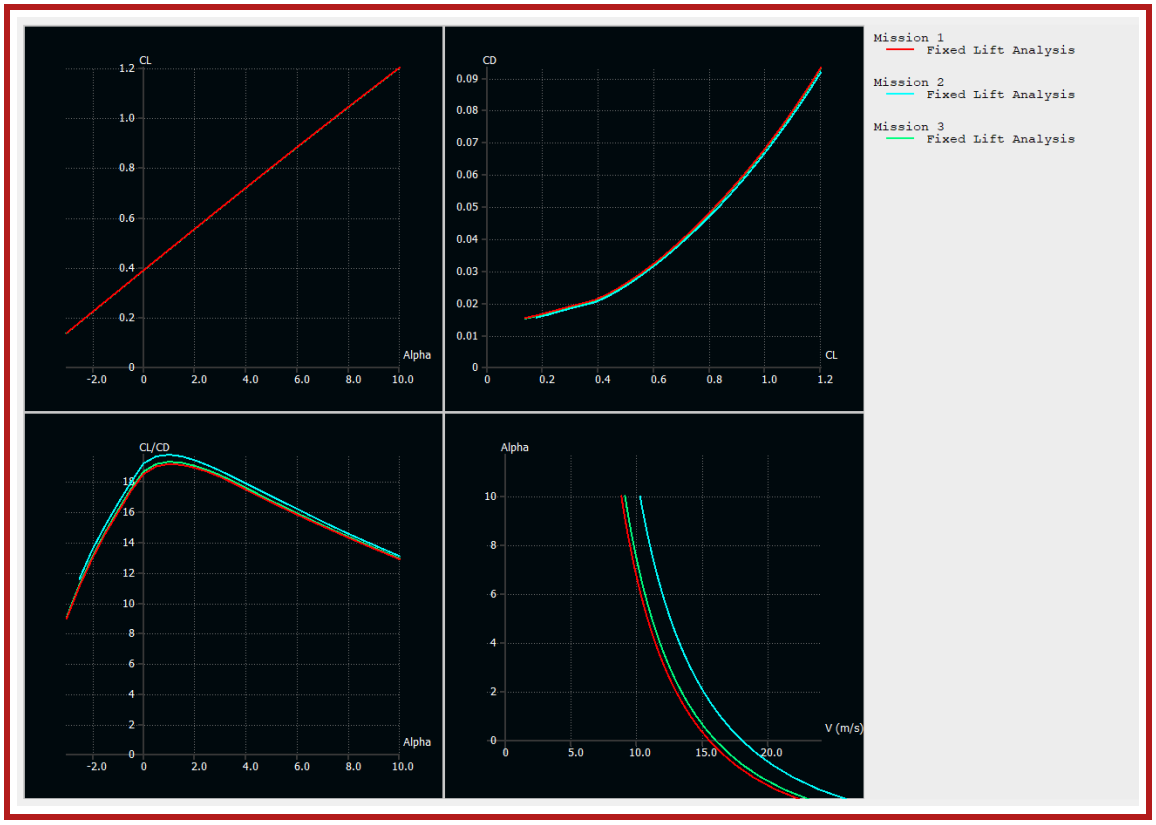

Figure 4.5.1: Expected aerodynamic performance for all flight missions. Clockwise from top left: C_L vs α, C_D vs C_L, α vs v, and C_L/C_D vs α

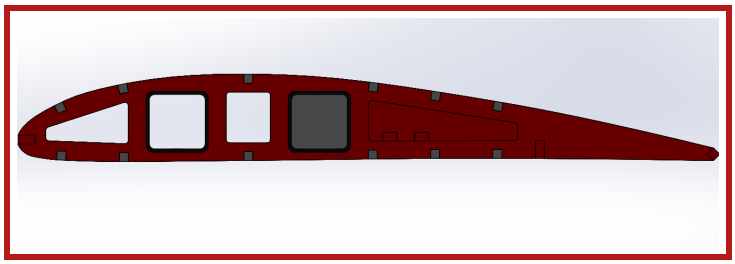

Figure 5.1.1: CAD Rendering of Wing Rib

and six hardwood ribs, while the rudder contains two balsa and four hardwood ribs. The horizontal and vertical stabilizers are connected to a baseplate. The vertical tail consists of four hardwood ribs and three balsa ribs. The thickness of the ribs, combs, stringers, and plates are all $1/8$" for the same structural and weight reduction reasons as for the wing. The vertical stabilizer is tapered for weight and drag reduction purposes. The horizontal stabilizer was not tapered to avoid moving the center of lift and center of gravity. The ribs at the root and tip and those attached to the servo are hardwood for structural integrity purposes. The ribs are connected by balsa stringers except for the hardwood ones on the leading edge. Two dowel rods (broken up to allow space for the rudder servo) run through the rudder ribs near the leading edge down to the baseplate to provide additional structural integrity. The rudder and elevators are attached to the tail using hinge points connecting hardwood comb structures on both ends of the point. One servo for the elevator and one servo for the rudder are installed in acrylic plates inserted into hardwood plates in the main tail body. Control rods connect the servos to control horns on the control surfaces. Only one elevator is connected to a servo, so

Parameter	Value
Airfoil	USA-35B
Wingspan	63.5 in
MAC	9.78 in
Wing Planform Area	621.03 in^2
Aspect Ratio	6.49
Sweep Angle	0 degrees
Taper Ratio	1
Angle of Incidence	0 degrees
Dihedral Angle	7 degrees
Aileron Span	2 x 23.77 in
Aileron MAC	2.47 in
Aileron Surface Area	117.42 in^2

Table 5.1.1: Final Wing Design Parameters

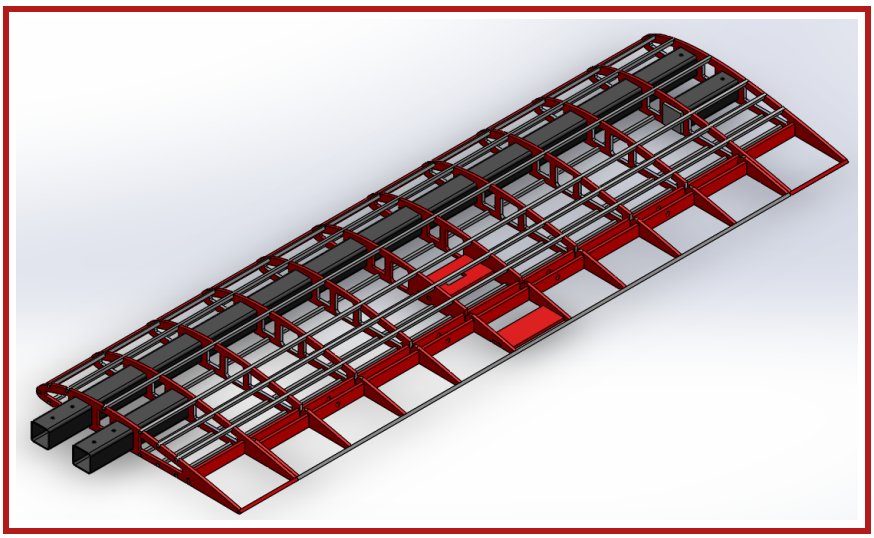

(a)

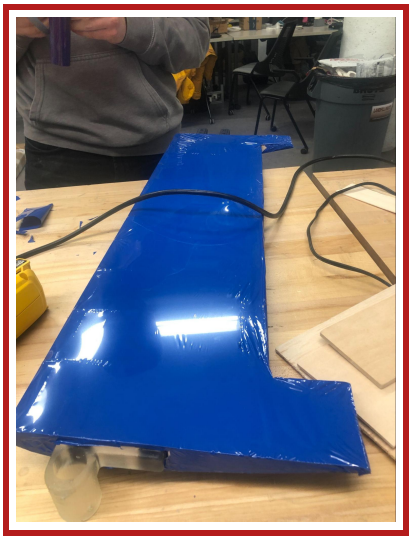

(b)

Figure 5.1.2: Finalized wing design. Figures 5.1.2a and 5.1.2b depicts a SOLIDWORKS render of a right-wing and the first iteration manufactured wing (prior to aileron attachment) respectfully. The design is mirrored for the left wing.

the two elevators are connected by a stringer and dowel rod so that they move together in the same plane. A hardwood T-plate was additionally added at the back of the baseplate to maintain the perpendicular angle between the horizontal and vertical stabilizers as to avoid “fluttering” of the empennage during flight. Figure 5.1.3 show CAD models of the final tail design.

5.1.3 Tail Integration Piece Detailed Design

The aircraft structure requires that an integration piece connecting the empennage and the longitudinal (tail) spar. The team decided that the design for the integration piece should be derived from the 2021-22 design. That is, it should be based on two carbon fiber L-brackets stabilizing the empennage connection to the tail spar.

The team found no meaningful issues with the previous design, but small improvements could be made.

Parameter	Value
Aerodynamic Configuration	Conventional Tail
Airfoil	NACA 0010 in
Horizontal Stabilizer speed	17.78 in
Horizontal Stabilizer Chord	6.39 in
Horizontal Stabilizer Planform Area	113.61 in^2
Horizontal Stabilizer Aspect Ratio	2.78
Elevator Chord	1.78 in
Vertical Stabilizer Span	7.09 in
Vertical Stabilizer Root Chord	5.34 in
Vertical Stabilizer Tip Chord	3.66 in
Vertical Stabilizer MAC	4.50 in
Vertical Stabilizer Planform Area	36.27 in^2
Vertical Stabilizer Aspect Ratio	1.33
Vertical Stabilizer Taper Ratio	0.69
Rudder Chord	2.39 in

Table 5.1.2: Final Tail Parameters

The team decided to use a design that kept the L-brackets as two separate pieces, but with the addition of a U-channel to unify the two pieces. The U-channel adds more stability to the integration by keeping the L-brackets firm, and translates to a more stable empennage. Additionally, instead of carbon fiber, this design would be made out of 3D printed material, due to its specific dimensions.

In calculating the factor of safety for the integration piece, the team determined that it would be under loads from the tail and tail spar (estimated to be 0.15 lbs and 0.22 lbs respectively). Using ANSYS, the maximum normal stress values for the design's geometry were obtained, utilizing the free-body diagram depicted in Figure 5.1.4b. The maximum normal stress was calculated to be 11.4 psi. Given the yield stress for Formlabs resin to be 9400 psi and the yield stress for Onyx filament to be 5800 psi[11], two potential materials, the factors of safety for the integration piece made from both materials is given by Equation 13. Both materials yield large factors of safety of over 500. Due to the high safety factors, there was very little concern about the device failing with either material. Regardless, Formlabs resin was decided to be used for Iteration I of the aircraft.

$$FOS = \sigma_y / \sigma_{applied} \tag{13}$$

One possible complication with the integration piece design involves a possible risk that when the integration piece becomes more worn, there will be some "play" between the L-brackets and the U-channel holding the pieces together. However, this instability will likely occur after a long time of use (i.e., many flight tests); not long enough to be an issue for this year.

5.1.4 Fuselage Detailed Design

The fuselage is designed with the overall objective of supporting mission payloads while remaining both structurally strong and light. It is also designed to integrate the necessary electrical components in a secured and geometrically aerodynamic manner to minimize drag during takeoff and flight. The geometry of the fuselage must be robust enough to hold all necessary components and integrate the wing and tail of the aircraft.

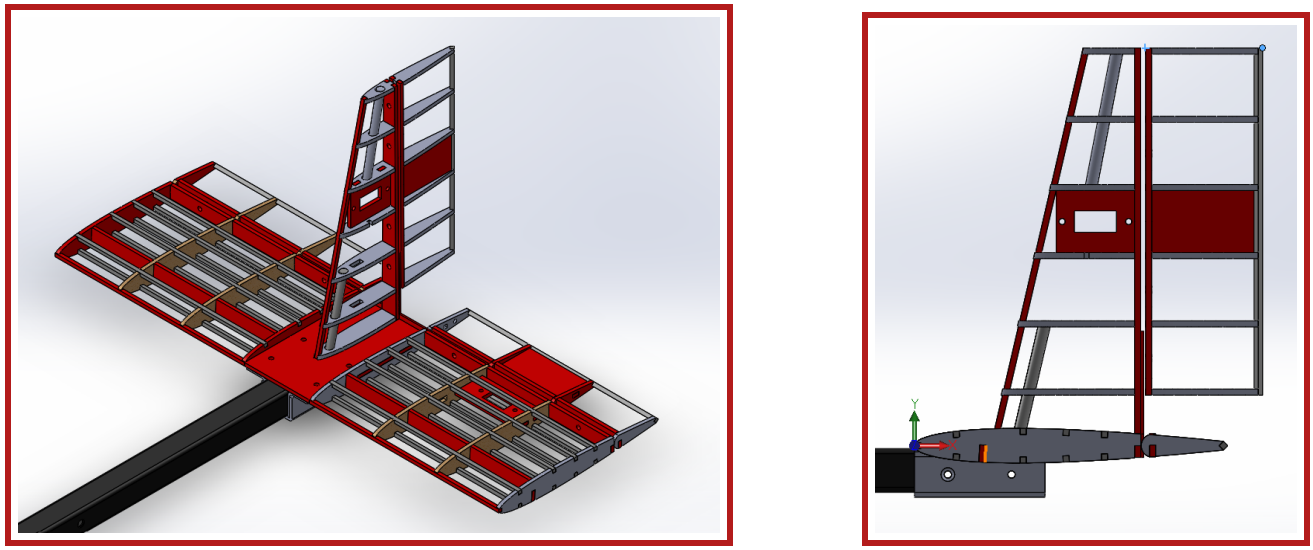

(a) (b)

Figure 5.1.3: Finalized tail design. Figures 5.1.2a and 5.1.2b depict SOLIDWORKS renders of the tail from an isometric and side view respectively.

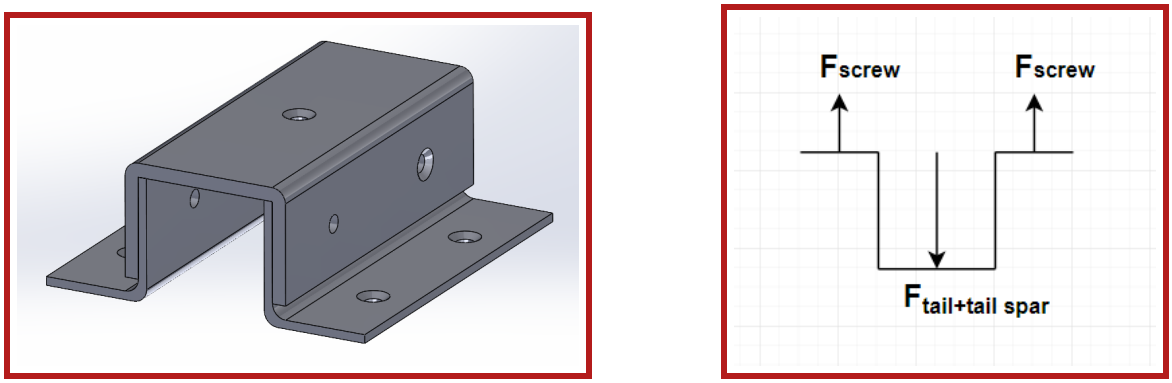

(a) (b)

Figure 5.1.4: CU DBF's tail-integration piece. 5.1.4a depicts a CAD model, while 5.1.4b depicts the relevant free-body diagram where $F_{\text{tail+tail spar}} = 0.3745lbs$

The general structure of the fuselage is made of a series of wooden ribs. A mixture of balsa and hardwood is used to balance strength and weight. Hardwood is used for the ribs at the nose and tail, as well as for pieces surrounding the wing integration and landing gear locations to provide the necessary strength to bear associated loads. The rest of the ribs were made out of balsa to lower overall weight. The center of the ribs is removed to form an internal cargo space. This opening extends into the tapered section to provide access to electronic components. The nose and tail ribs are solid, however, save for holes for the fuselage and tail spars.

Balsa wood stringers $1/8$" thickness and $1/4$" wide run the span of the plane and are secured on the outside of the ribs using notches to provide increased surface area for MonoKote application, thus improving the aerodynamic structure of the fuselage. Towards the center of the fuselage, ribs have one of their sides removed to accommodate a hatch. (MECH 4) The middle section of the fuselage is straight in order to hold mission payloads. These ribs include small notches so they can be easily aligned with a baseplate. The nose

and tail sections are tapered in order to improve aerodynamics and reduce flow separation. Figures 5.1.5 and 5.1.6 depict the general fuselage rib design and side profile respectively.

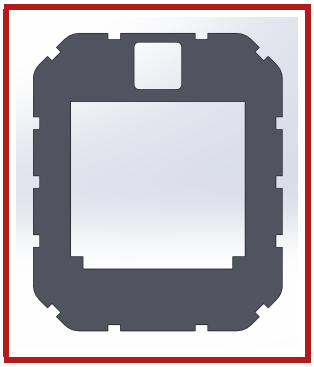

Figure 5.1.5: Fuselage Rib Profile

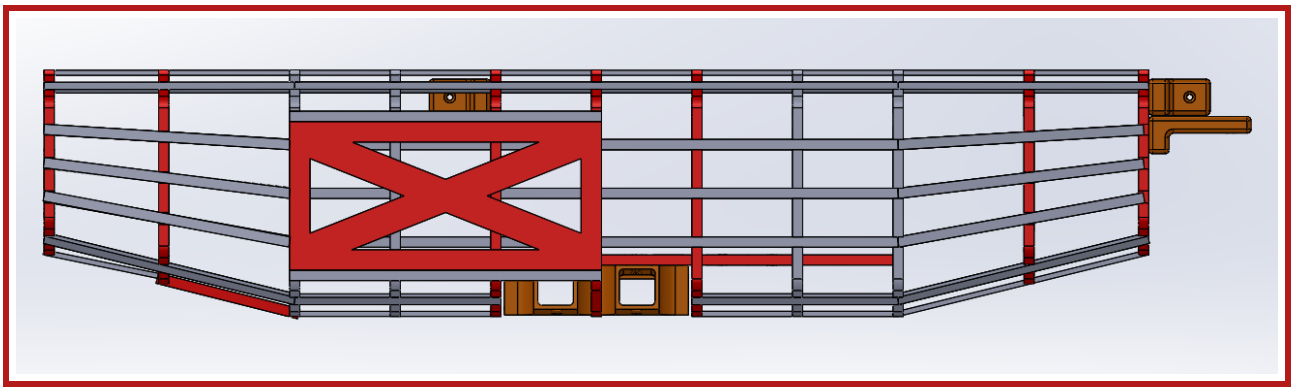

Figure 5.1.6: Fuselage Side Profile

In addition to supporting the tail, a carbon fiber spar was added to span the length of the fuselage. This adds significant structural strength to the semi-monocoque fuselage design. The spar attaches to the ribs through two 3D printed L-brackets. It was found that Onyx filament, a nylon-based material with chopped carbon fiber, fit the needs best. It is the strongest and lightest filament on hand, with a tensile strength of 5800 psi, and a density of $74.9lb/ft^3$. These screw into the fuselage through holes in the ribs and connects to the spar through a removable pin to ease assembly. Fuselage ribs have square cutouts to match the profile of this piece, allowing the spar to also provide torsional stability to the rest of the structure. Figure 5.1.7 depicts the bracket as well as its location in the fuselage.

A hardwood baseplate $1/4$" thick was fitted to the bottom of the ribs to hold the Mission 2 payload battery, and also provide additional structural support for the fuselage. Hardwood was used to ensure that the baseplate would not warp under forces from the payload and landing gear. The baseplate has screw holes to connect the wing integration pieces and landing gear. Notches are etched into the sides of the baseplate to provide a flush interface with the ribs and ensure both accurate spacing and structural strength.

The integration between wing and fuselage is a vital part of any aircraft. It is necessary that this junction be extremely strong to withstand the lift forces generated by the wings during flight. This is exacerbated by the fact that this year's DBF competition has a ground test mission designed to specifically test the strength of the wings and wing integration, as well as a need for the wings to be modular.

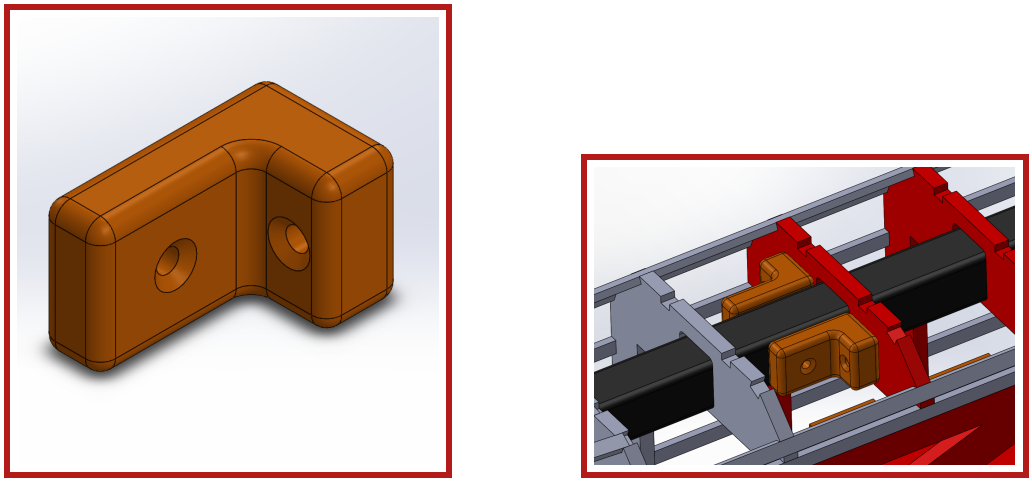

(a) (b)

Figure 5.1.7: Spar integration bracket. Figure 5.1.7a depicts the position of the integration piece from a bottom-view, and Figure 5.1.7b shows the CAD render of the piece.

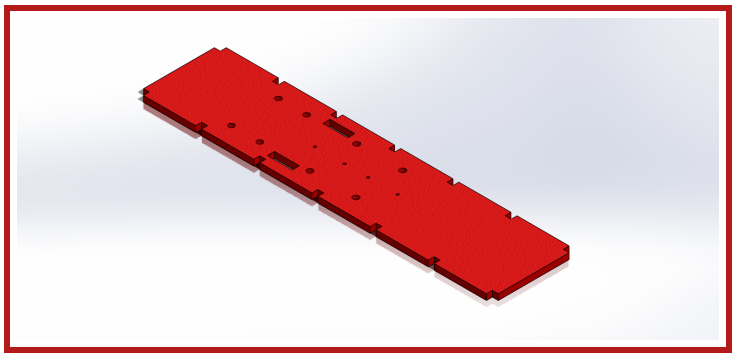

Figure 5.1.8: Fuselage Baseplate

The ground test requires that the wing integration is able to withstand a large load. With the Aerodynamics and Controls subteam settling on a low wing consisting of two main spars, the two wing integration pieces sit under the base plate and connect a bottom fuselage spar to the wing spars. The piece screws permanently into the fuselage spar, while locking into the wing spars using clevis pins. This pin design allows for a quick and easy installation of the wings during the competition.

A seven-degree dihedral angle is implemented as shown in figure 5.1.9. There were also concerns about the strength of the wing integration pieces which were addressed by extending the top to the base plate of the aircraft. In order to ensure that this dihedral would not cause the wing or wing spars to interfere with the fuselage baseplate or ribs, the slots for the wing spars are extended to provide clearence.

It was decided that the key parameters for this component were strength, cost, manufacturability, and weight. Strength is the most important of these parameters because it needs to be able to handle heavy wing tip loads, particularly during the ground mission. Manufacturability was also weighted highly due to the importance of rapid prototyping in our design process.

As with the spar-integration brackets, it was decided that Onyx filament would be the best material for the wing integration piece due to its high strength and low weight. While aluminum is strong, it is much heavier than Onyx and is not nearly as manufacturable. Likewise, carbon fiber was ruled out as it would be required

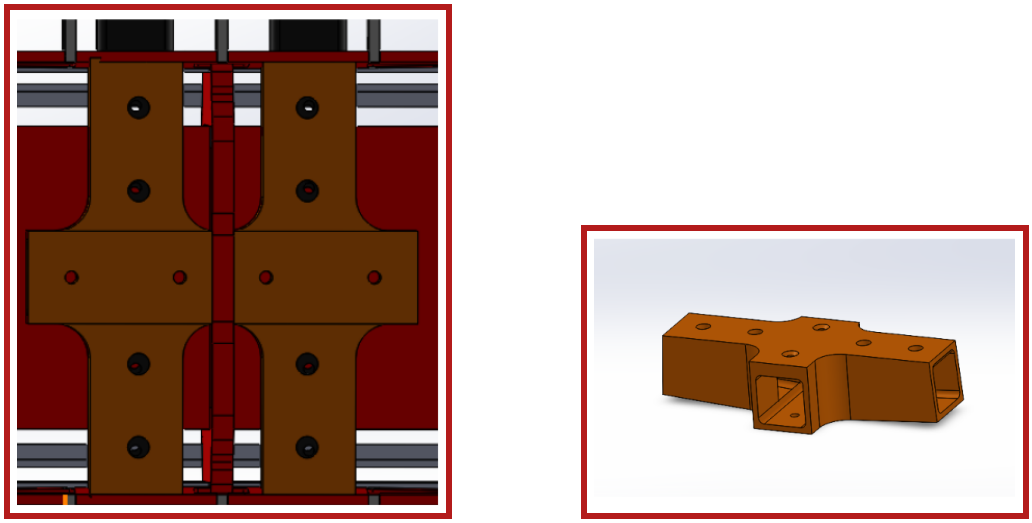

(a) (b)

Figure 5.1.9: Wing integration piece. Figure 5.1.9a depicts the position of the integration piece from a bottom view, and Figure 5.1.9b shows the CAD render of the piece

to get a third party to manufacture the part, leading to long wait times and very high costs.

To integrate the tail spar with the fuselage, a 3D-printed tube serves as the tail integration adapter. This piece connects to both the rear rib and the spar running through the fuselage. The tube provides two strong points of contact to reduce the deflection of the tail during flight. Onyx filament is once again used in order to sustain the torques generated by the control surfaces on the tail. The tube is screwed into the rear rib and the fuselage spar and is pinned into the tail spar to accelerate the installation process. Figure 5.1.10 depicts this design.

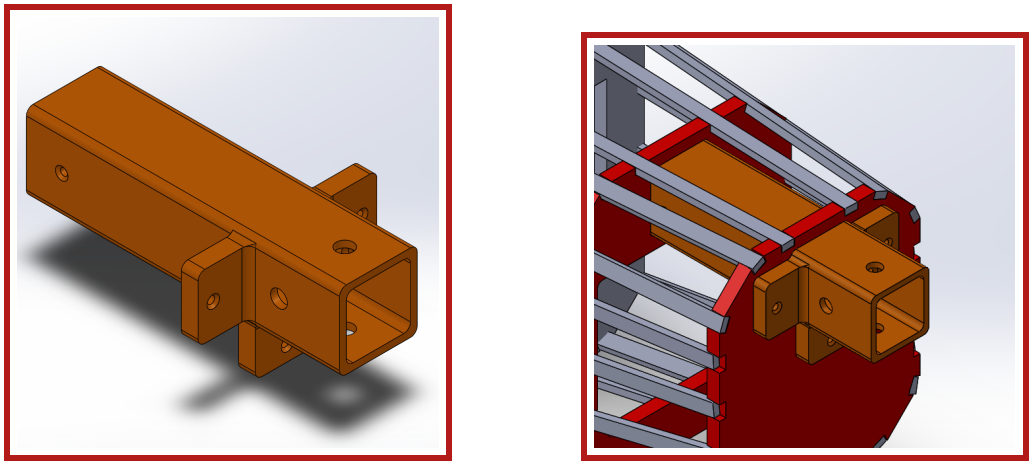

(a) (b)

Figure 5.1.10: Tail integration tube. Figure 5.1.10a depicts the position of the integration piece from an isometric view, and Figure 5.1.10b shows its integration with the fuselage.

5.1.5 Landing Gear Detailed Design

After deciding the placement of the battery, the Mission 2 electronics package, and the Mission 3 jamming antennas, the center of gravity for each mission was determined and the back landing gear was placed slightly behind the center of gravity furthest from the front of the plane. Both the front wheel and the back landing gear integrates into the fuselage in different ways that minimizes the shock from the impact to the rest of the aircraft and prevents critical damage to the fuselage. Specifically, the front wheel integrates into the fuselage using a nose plate that is slotted between two ribs. This allows the front wheel to absorb shock from the aircraft landing. The back landing gear connects to the fuselage's baseplate using four threaded screws. These screws connect the fuselage to an integration plate separated by four springs. Based on the preliminary testing, these springs are necessary because directly connecting the back gear to the fuselage made the baseplate prone to breaking during landing. As a result, the springs serve to reduce the shock passed to the aircraft and dissipate the vertical momentum of the plane upon landing (MECH 7). The back integration piece holds the remaining components of the back gear such as the carbon fiber pieces and the wheels.

The height of the landing gear was greatly taken into consideration because of the effect it would have on the aircraft's stability and drag. The primary factor that led to a height of 6.3 inches for the back landing gear, was the stability of the aircraft during landing (MECH 6, 7). A smaller landing gear on previous aircraft constructed by the team caused the aircraft to sway upon landing, putting it at risk of hitting the ground. To correct this issue, the width of the landing gear needed to increase, however, this requires increasing the height proportionally. As a result, two small carbon fiber pieces are used rather than a single connected piece. This allows the team to adjust the width of the rear landing gear by moving the pieces on the integration piece instead of relying on the dimensions of the conventionally arched pieces. This leads to an overall wider profile while maintaining a reasonable landing gear height.

The front landing gear was chosen because of its durability, stability, and its shock absorbance characteristics. It includes an attached servo to help steer the plane during takeoff and landing, helping it adapt to any major deviations in the runway (MECH 6). The separability in an effort to make the takeoff and landing stages of flight more reliable and it gives the pilot significantly more control of the aircraft without adding complex mechanisms such as brakes. Because of a long maximum take-off and landing distance, through testing, it was determined that braking was not necessary because the aircraft could come to a complete stop (MECH 7). However, it was noted that if the aircraft was not perfectly straight on the runway, a possible deviation would be exacerbated as the takeoff distance increased, thus increasing the need for a steerable front gear.

5.1.6 Mission 2 Electronics Package Detailed Design

The Mission 2 payload was designed to be easily secured into the fuselage and provide sufficient structures for the contained weight. The overall shape of the package is rectangular to easily fit inside the plane. Weights shifting in flight would lead to a dangerous load shift leading to instability. The box, therefore, includes two methods of securing itself to the baseplate. Extrusions from the bottom of the payload can slot into the fuselage, and velcro is attached to hold it in place. Additionally, the box was made to have a solid infill and holes that fit the dimensions of the weights being added. This was designed around cylindrical one kilogram weights that can easily be inserted into the package. To ensure that the weights remained in the package, a

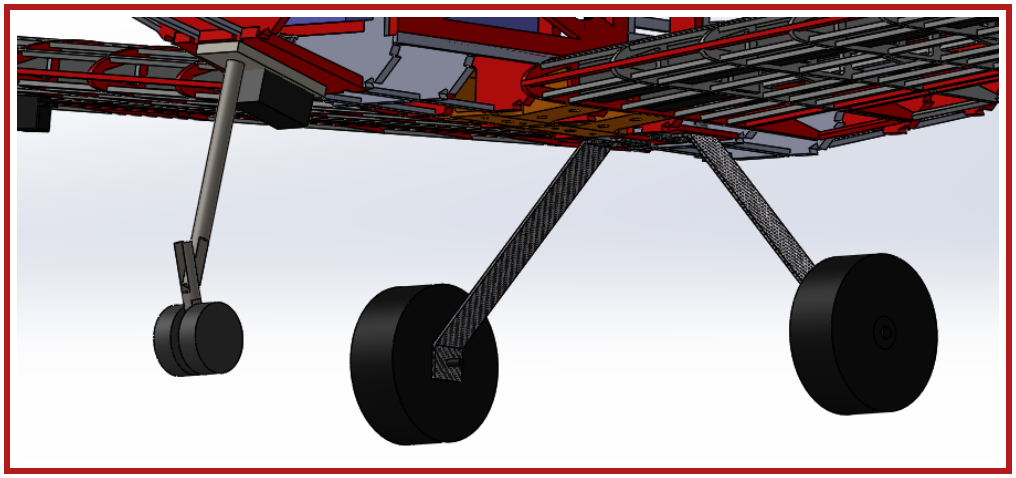

Figure 5.1.11: Landing Gear CAD Render

lid was designed to slot on top of the box.

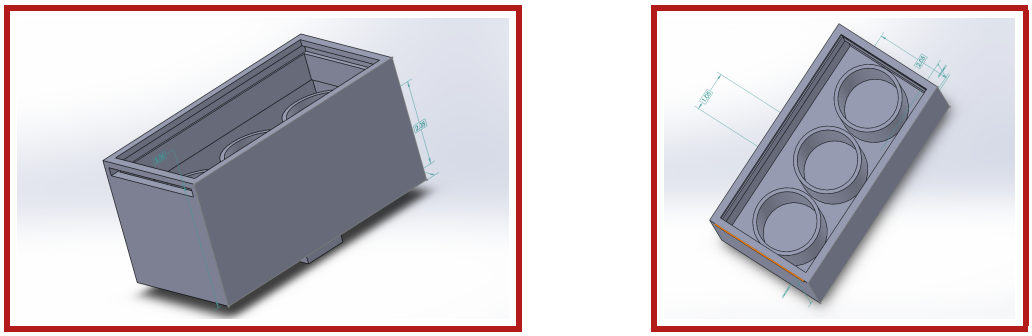

(a) (b)

Figure 5.1.12: Mission 2 package design. Figures 5.1.12a and 5.1.12b depict an isometric and top-view of the package respectively.

5.1.7 Mission 3 Integration Detailed Design

The final design of the Mission 3 integration piece consists of a pair of square inserts that slot into the wing spars, as well as a rounded protrusion into which a cylinder is cut to accommodate the PVC analog. To maintain the antenna's verticality while accounting for the dihedral of the wings, this cylinder is angled at seven degrees. A vertical hole is drilled into the spar inserts to match a No. 6 screw, which pass through both the inserts and the spar, and holds the assembly securely in place. Similar holes are drilled into the cylinder; one hole about 0.4 inches from the bottom, where a screw is inserted to prevent the antenna from moving vertically downwards, and two holes a similar distance from the top, which would apply pressure to the antenna in order to fully constrain the antenna.

Due to the decision made to minimize the weight of the integration piece, height was initially chosen to be consistent across the entire piece. This meant that it would only be as tall as was necessary for the inserts to take up the entire internal volume of the spars, and no taller. However, this consideration gave way to concerns about the stability of the antenna, which would only be secured along the small area allowed by this constraint. As a result, a cylindrical extension was created around the antenna, raising the height at this area

to 1.7 inches and more than doubling the area available for securing it.

During materials selection, the team considered several types of plastic, as well as wood and aluminum. The latter two were quickly discarded due to the difficulty of precise woodworking and the weight associated with any metal part. In contrast, choosing a plastic meant that the team could take advantage of additive manufacturing for precise and intricate designs while not sacrificing either weight or strength. Out of the many options available to the team, resin was eventually selected due to its excellent strength, as well as a greater resistance to shearing forces compared to choices such as Onyx or ABS. Additionally, it can be threaded comparatively easily for its strength, eliminating the need for the heat-set inserts other materials might require.

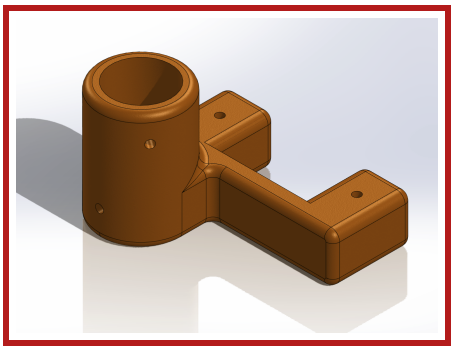

Figure 5.1.13: M3 Integration Adapter CAD Render

5.1.8 Ground Mission Detailed Design

The final design of the ground mission supports consists of two pillars made of lasercut ¼" plywood slotted together and screwed together with L-brackets to ensure stability. There is a 3D printed part screwed into the top where the plane rests, and a ½" schedule 40 PVC pipe is inserted through the Mission 3 adapter to prevent wood buckling. This design was made by testing of the static structural stability of plywood and PVC to ensure they would hold the airplane's weight. The plywood is optimal due its ability to withstand associated loads and because of its low cost. The PVC pipe was added to provide a greater factor of safety against material failure in the wooden components. Figure 5.1.14 depicts the finalized design.

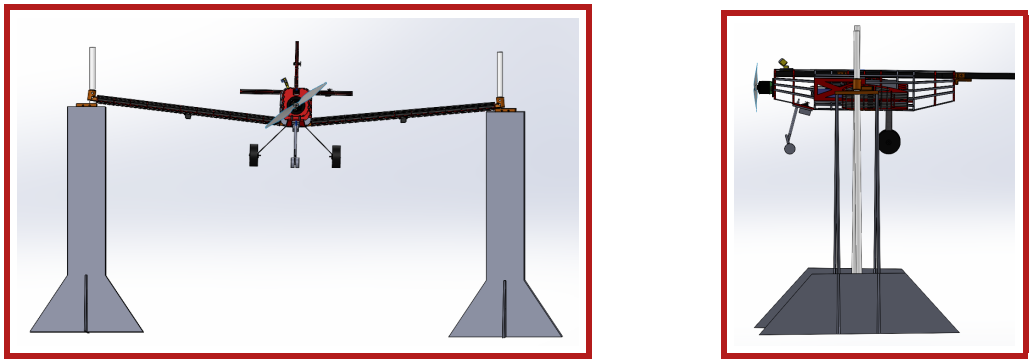

(a) (b)

Figure 5.1.14: Ground mission stand design. Figures 5.1.12a and 5.1.12b depict a SOLIDWORKS visualization of a front and side-view of the design respectively.

5.1.9 Propulsion Detailed Design

A single Admiral 4500mAh lithium-polymer battery provides power to the propulsion system necessary to sustain flight for all three flight missions. The battery's placement varies between missions from the front of the fuselage to closer to the center, in order to maintain the plane's center of mass (AVIO 4). A single tractor propulsion system serves as the propulsion configuration, consisting of a Cobra C-4120/22 motor paired with an APC 12x7 propeller to provide thrust to the aircraft. An external arming plug is also mounted to satisfy AVIO 5. Table 5.1.3 depicts the major components used for the propulsion system. This system is used for all three flight missions.

Component	Details
Battery	One Admiral 4500mAh 6s 80C LiPo
ESC	One Cobra 60A ESC
Motor	One Cobra C-4120/22 430Kv Brushless Motor
Propeller	One 12x7 APC Propeller

Table 5.1.3: Final Propulsion System Configuration

The motor is mounted on the front of the fuselage. It is secured to the fuselage via two motor mounts: one that came with the motor, and one that was 3D printed (PROP 4). The manufacturer's included motor mount presented both integration issues and insufficient stability, so a second mount was printed from Onyx (Figure 5.1.15). A circular plate design allows the shaft and wires to run through the center of the plate into the fuselage. Four #8 holes were added to allow the motor to be properly secured to the fuselage. Tests will be performed on this piece to ensure that it can endure stresses produced by the motor.

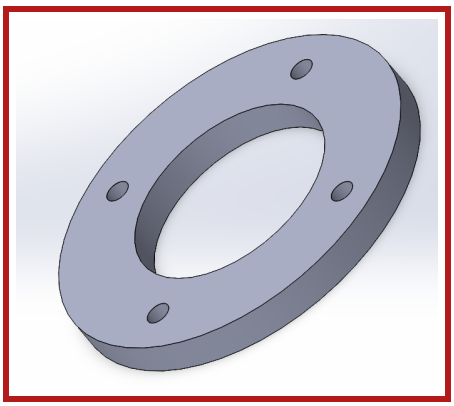

Figure 5.1.15: CAD Render of the Motor Mount

In addition, all control surfaces are actuated by Futaba S3114 servos that are connected to a Spektrum 8-channel receiver and is controlled by a Spektrum DX-8e transmitter. The receiver itself is separate from the propulsion system, thus a separate NiMH battery fitted with an external switch is used to power the receiver (AVIO 5). Figure 5.1.16 depicts the wiring diagram of the aircraft.

5.2 Weight and Balance

As the total mass of the aircraft as well as the positioning of certain loads change between each mission, calculations were performed in order to ensure the best center of mass to maximize aircraft performance.

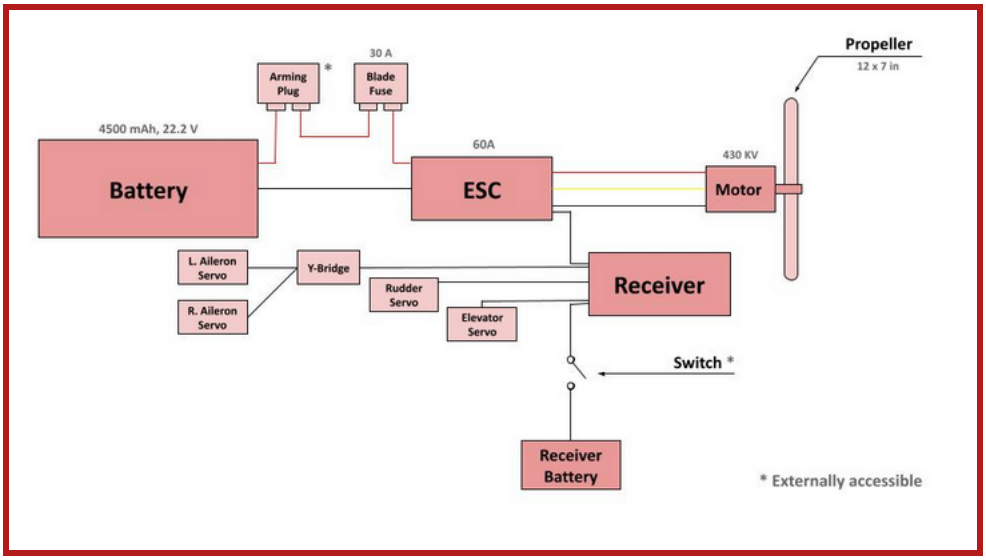

Figure 5.1.16: Diagram of Electronics System

From the stability analysis found in section 4.4.1, the center of gravity needed to be 3.48 inches aft of the leading edge of the aircraft. The neutral point was found to be 5.16 inches aft of the leading edge. As the battery contributes significantly to the mass of the plane, it will have to be positioned differently for each mission. The center of mass of each component of the aircraft was determined using SOLIDWORKS. All center of gravity values is taken using a reference point set at the centerline of the baseplate of the fuselage, even with the leading edge of the wing. The x-axis is defined aftward along the fuselage of the aircraft, the y-axis is defined along the vertical height of the aircraft, and the z-axis is defined along the left wing. Table 5.2.1 displays the estimation for the location and magnitude of the center of gravity of each component of the aircraft.

5.3 Aircraft Performance

As the detailed design is derived from the preliminary design, the expected aerodynamics performance and mission performance has not changed. XFLR5 serves as the team's primary software to run lift, drag, and static and dynamic stability simulations. From there, the team is able to estimate mission flight speeds and thus expected mission flight times. Sections 4.5 and 4.6 explain in detail how these performances are calculated. Table 5.3.1 describes the expected aircraft performance and parameters.

5.4 Drawing Package

Component	Mass (lbs)	CG_x (in)	CG_y (in)	CG_z (in)
All Missions				
Fuselage	1.16	4	1.3	0
Front Landing Gear	0.176	-5.92	-3.28	0
Back Landing Gear	-0.238	7.01	-3.77	0
Wing	0.640	4	0	0
Tail	0.220	38.31	4.42	0
Motor	0.639	-11.35	1.75	0
Propeller	0.055	-12.85	1.75	0
ESC	0.132	-2.25	-1.324	0
Mission 1				
Battery	1.44	3.48	0.805	0
Total	4.70	5.16	0.85	0
Mission 2				
Battery	1.44	0	0.805	0
M2 Load	2.65	5.225	1.525	0
Total	7.35	5.16	0.88	0
Mission 3				
Battery	1.44	3.48	0.805	0
M3 Load	0.22	3.48	-5.58	$\pm$31.5
Total	4.92	5.16	1.16	0

Table 5.2.1: Weight and Balance for BR-23: Vermillion

Variable	Meaning (units)	Performance, empty (M_1)	Performance, MTOW (M_2)	Performance, antenna (M_3)
m	Mass (lbs)	4.70	7.35	4.92
$C_{L,cruise}$	Coefficient of lift under cruise conditions	0.56	0.56	0.56
$C_{D,cruise}$	Coefficient of drag under cruise conditions	0.03	0.03	0.03
L/D_{cruise}	Lift-to-Drag ratio under cruise conditions	18.67	18.67	18.67
V_c	Cruise speed (ft/s)	42.65	53.34	44.00
$t_{mission}$	Time to complete each mission (min)	3.52	10.0	3.41
-	Mission specific parameters	-	2.645 lbs	6 in

Table 5.3.1: Expected aerodynamic and mission performance for each mission

FRONT VIEW

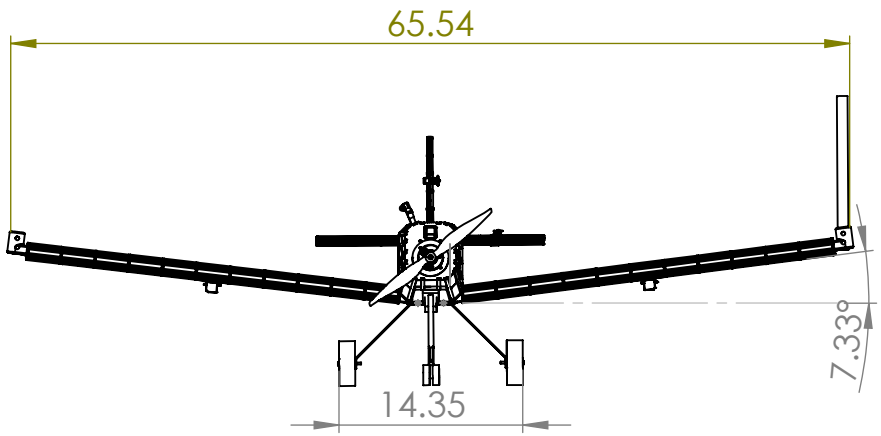

ISOMETRIC VIEW

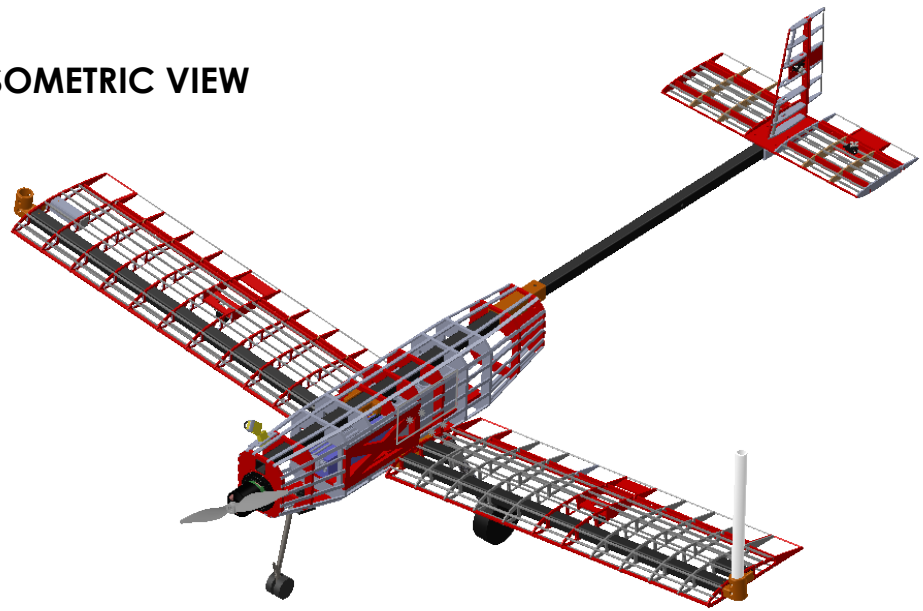

TOP VIEW

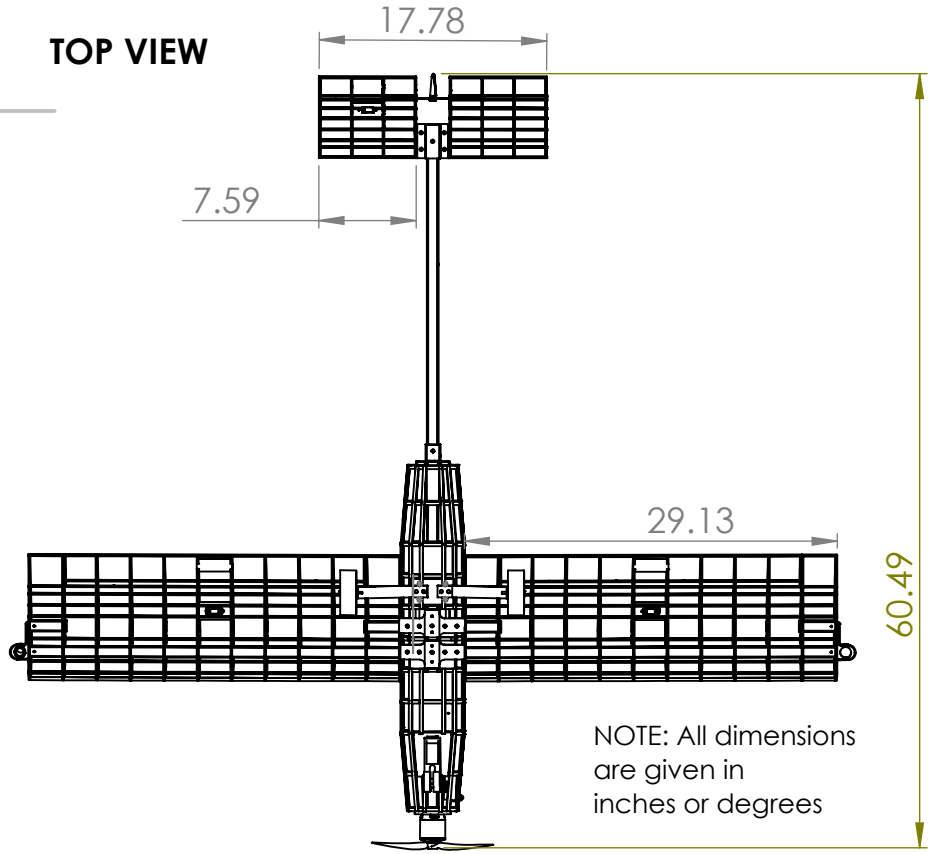

LEFT VIEW

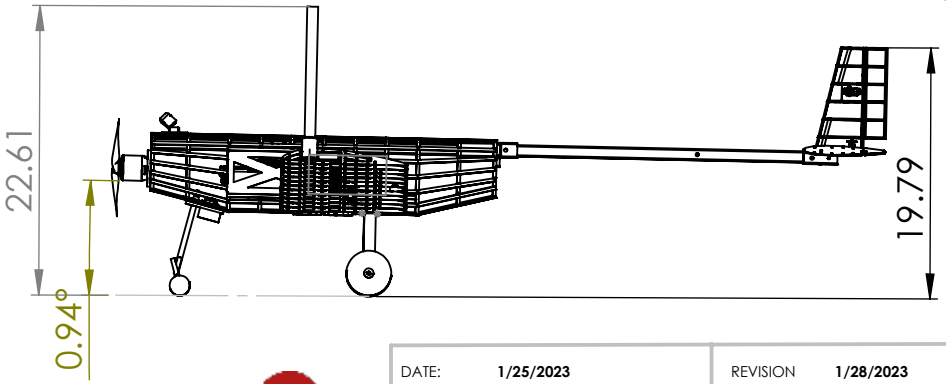

cuDBF

DATE: 1/25/2023 | REVISION 1/28/2023

Cornell University

TITLE: Three-View Drawing

DRAWN BY: Neil Ramasray

CHECKED BY: Adrian Lee

313 Campus Rd. Ithaca, New York 14853

A

WEIGHT:

SCALE: 1:15

ALL UNITS ARE IMPERIAL [IPS]

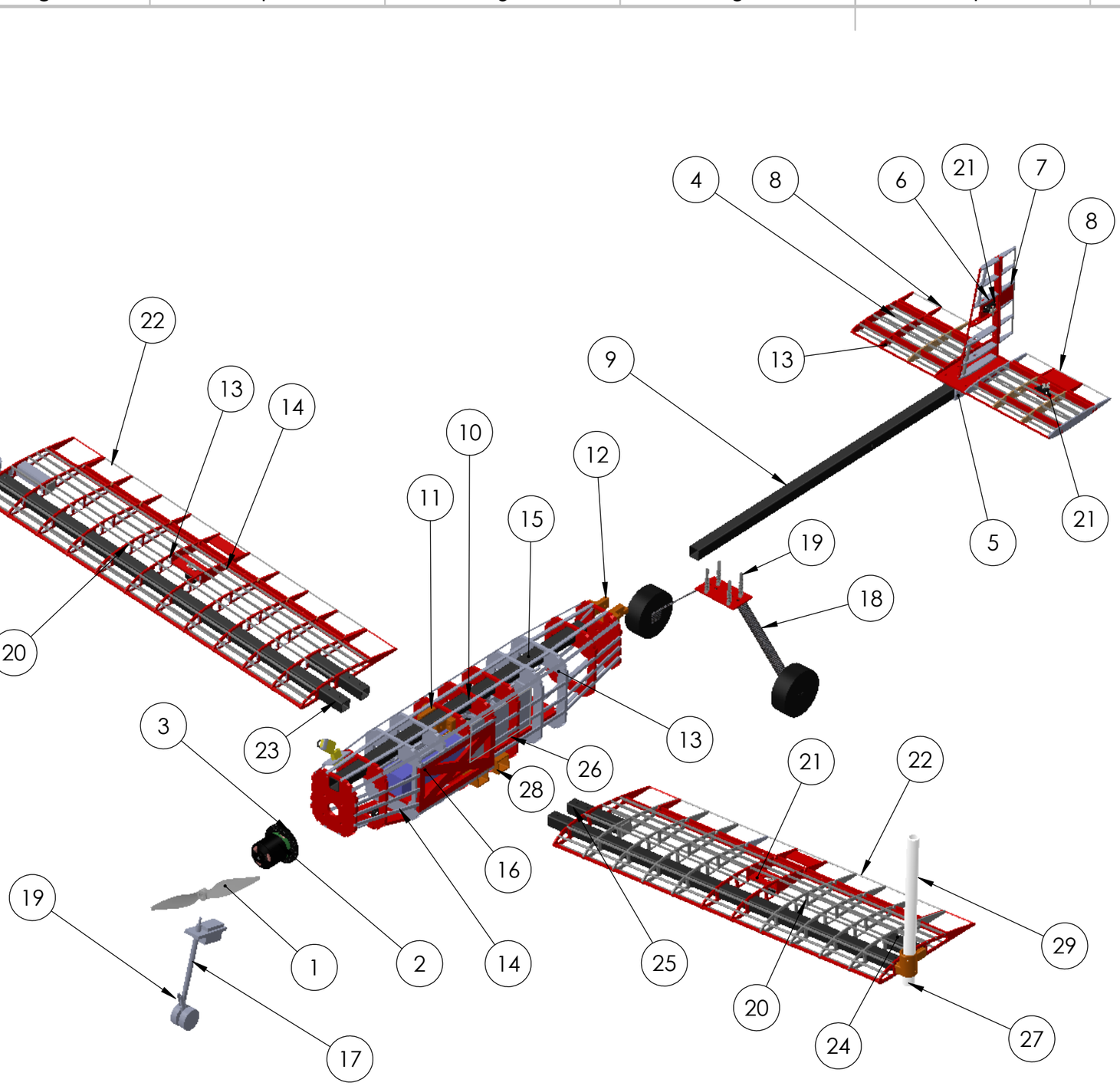

ITEM NO.	PART NAME	MATERIAL	QTY.
1	Propeller	APC	1
2	Motor	Cobra C-4120/22	1
3	Motor Mount	Hardwood / Onyx	1
4	Horizontal Stabilizer	Balsa / Hardwood	1
5	Horizontal Stabilizer Mount	Hardwood	1
6	Vertical Stabilizer	Balsa / Hardwood	1
7	Rudder	Balsa / Hardwood	1
9	Tail Spar	Carbon Fiber	1
10	Fuselage	Balsa / Hardwood	1
11	Fuselage Spar L-Brackets	Onyx (CF Nylon)	2
12	Tail Spar L-Brackets	Onyx (CF Nylon)	3
13	Ribs	Balsa / Hardwood	50
14	Stringers	Balsa / Hardwood	62
15	Upper Fuselage Spar	Carbon Fiber	1
16	Fuselage Hatch	Hardwood	1
17	Front Landing Gear	PLA / Aluminum	1
18	Rear Landing Gear	CF / Hardwood	1
19	Landing Gear Suspension Springs	Stainless Steel	5
20	Wing	Balsa / Hardwood	2
21	Servo Bracket	Resin	5
22	Aileron	Balsa / Hardwood	2
23	Main Wing Spar	Carbon Fiber	2
24	Antenna Wing Spar	Carbon Fiber	2
25	Fuselage Wing Spar	Carbon FIber	2
26	Lower Fuselage Spar	Carbon Fiber	1
27	Antenna Adapter	Resin	2
28	Wing Integration Adapter	Onyx (CF Nylon)	2
29	Antenna	PVC	1

NOTE: All dimensions are given in inches or degrees

Cornell University Design Build Fly

cuDBF

DATE: 2/1/2023 | REVISION 2/4/2023

Cornell University

DRAWN BY: Neil Ramasray

CHECKED BY: Adrian Lee

TITLE:

Structural Arrangement

313 Campus Rd. Ithaca, New York 14853

A3

WEIGHT: 6.03 pounds | SCALE:1:10 | ALL UNITS ARE IMPERIAL [IPS]

Cobra 60A ESC

Admiral 4500mAh 6S 22.2V
40C LiPo Battery

Spektrum Receiver

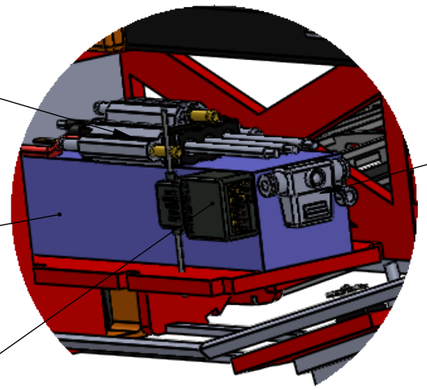

Inner Electrical Components

SCALE 2 : 5

MAXI Fuse Holder

Arming Plug

SCALE 2 : 5

Futaba Servo

SCALE 3 : 5

Rudder Servo

Elevator Servo

Cobra C-4120/22
Brushless Motor

Aileron Servo

Front Gear Servo

Aileron Servo

NOTE: All dimensions are given in inches or degrees

Cornell University Design Build Fly

DATE: 2/6/2023	REVISION 2/9/2023

Cornell University

TITLE: Systems Layout

DRAWN BY: Neil Ramasray

CHECKED BY: Adrian Lee

313 Campus Rd. Ithaca, New York 14853

A3

WEIGHT: 6.03 pounds

SCALE:1:5

ALL UNITS ARE IMPERIAL [IPS]

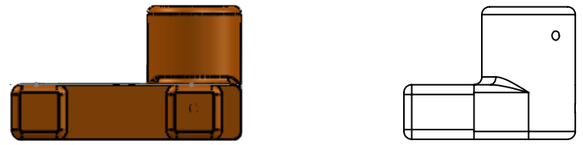

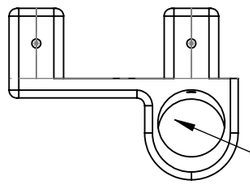

Antenna Hole

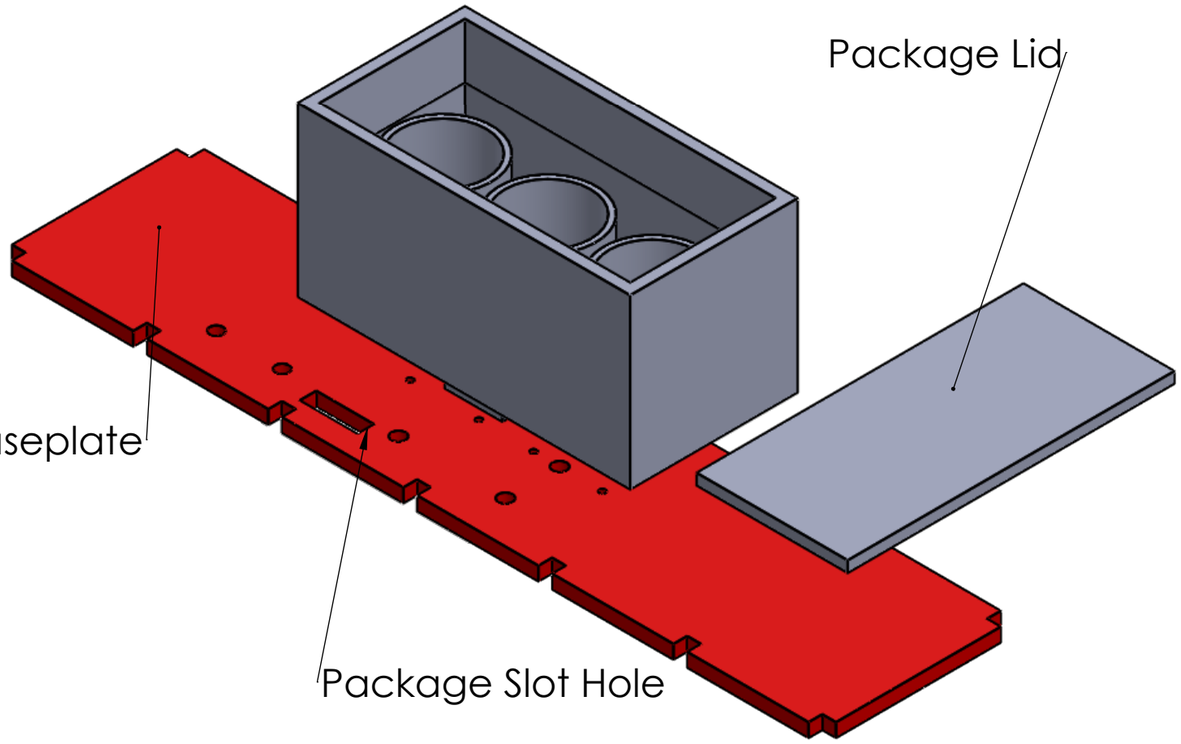

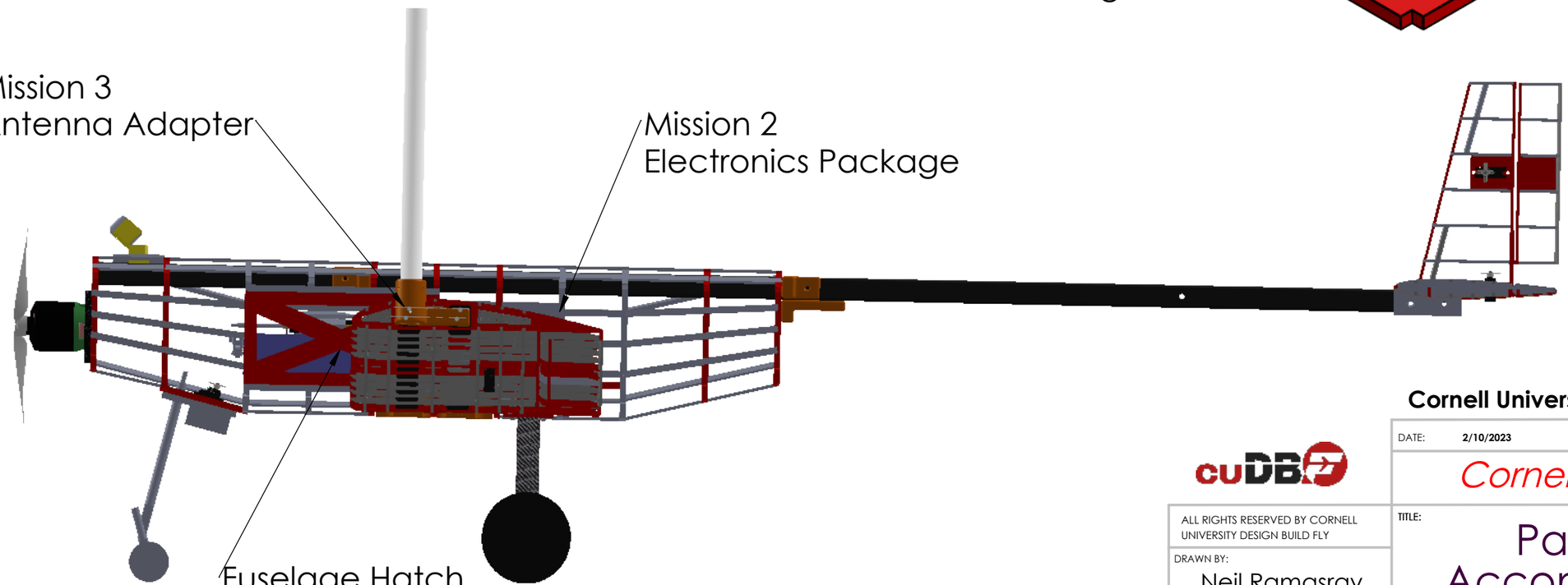

NOTE: All dimensions are given in inches or degrees

Cornell University Design Build Fly

DATE: **2/10/2023** REVISION **2/14/2023**

Cornell University

DRAWN BY: Neil Ramasray

CHECKED BY: Adrian Lee

TITLE: **Payload Accomodation**

313 Campus Rd. Ithaca, New York 14853

A3

WEIGHT: 6.03 pounds

SCALE:1:5

ALL UNITS ARE IMPERIAL [IPS]

6 Manufacturing Plan

6.1 Workflow

The team has a manufacturing process resembling that of the design, build, fly iteration cycle. The process goes through different phases, starting with modeling, then fabrication, then subsystem and system assembly, and ending with analysis and testing. This is depicted in Figure 6.1.1. After the competition rules release, sizing and scoring analysis is performed to determine what parameters to optimize for the competition. After this optimization along with the initial conception of design, CAD models are developed using SOLIDWORKS to visualize how components would operate and integrate with one another. When completely designed and reviewed, the models enter the fabrication stage where they are converted into .dxf files to be lasercut, or .stl files to be 3D printed.

All manufactured parts, along with externally purchased components, are then moved along into the system/subsystem assembly phase, where they are assembled into their respective subsystem components. Materials such as balsa, hardwood, resin, carbon fiber, and other electrical components are integrated using epoxy, cyanoacrylate glue, wood glue, heat shrink tubes for wiring, or hardware fasteners including nuts, bolts, and screws. MonoKote, a smooth and continuous film, is used when necessary to cover subsystems/components that heat shrinks using a heating iron and a heat gun. During integration, if subsystems are not able to integrate smoothly, it may become necessary to revert back to component assembly, cycling back through the assembly process. This cycle is repeated multiple times in order to iterate on the most effective mission-based aircraft, with mission mechanisms being included in this process as well.

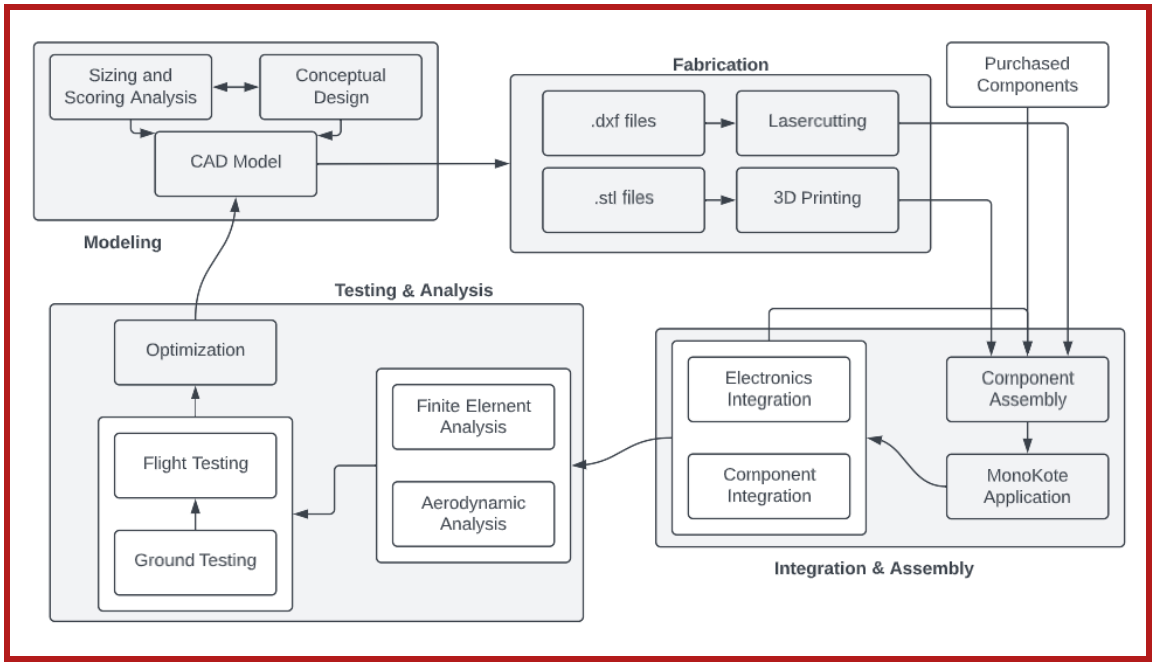

Figure 6.1.1: Manufacturing Flow Chart

6.2 Manufacturing Processes Investigated

Various manufacturing processes were considered for the build-up of the aircraft. The wings, empennage, fuselage, and mission-specific payloads and integration systems have various parameters that need to be considered whilst manufacturing. The following sub-section outlines some of these processes.

6.2.1 3D Printing

3D Printing allows for the fabrication of highly-complex parts not easily replicable. CU DBF has access to Cornell University Rapid Prototyping Lab (RPL), which houses several 3D printers that can be loaded with materials such as PLA, ABS, resin, and Onyx filament (a nylon-based filament with chopped carbon fiber). Figures 6.2.1 show some of the printers used for manufacturing.

(a) Stratys F370 ABS 3D Printer

(b) Fortus 250mc PLA 3D Printer

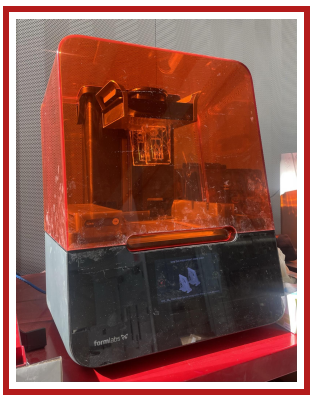

(c) FormLabs 3+ Resin 3D Printer

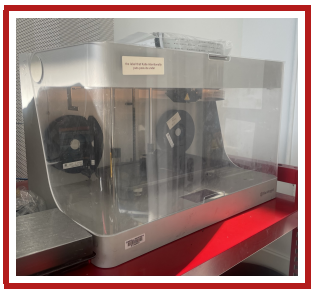

(d) Markforged Mark Two Onyx 3D Printer

Figure 6.2.1: The 3D printer CU DBF uses. All of these printers are located in the Cornell Rapid Prototype Lab.

6.2.2 Laser Cutting

With the mainframe of the aircraft consisting of primarily balsa and basswood, there are a number of precise parts that need to be cut out. CU DBF utilizes the laser cutters in the Rapid Prototyping Lab to ensure that parts are cut with pinpoint accuracy. The laser cutter shown in Figure 6.2.2 is able to cut large areas (36” x 24”) of wood up to a quarter-inch thick, making it extremely valuable for the team.

6.2.3 Adhesives

There are four different adhesives used to manufacture the aircraft: cyanoacrylate glue (CA), wood glue, epoxy, and Velcro. Cyanoacrylate is used to permanently bond balsa-to-balsa wood construction, including ribs and stringers. Wood glue serves as a stronger glue, useful when attaching other types of wood together (balsa to basswood, basswood to basswood). Epoxy is used to attach plastic and composite components together. Finally, Velcro is used a temporary adhesive for objects that need to shift around, namely, for the fuselage hatch, battery attachment, and mission two attachment.

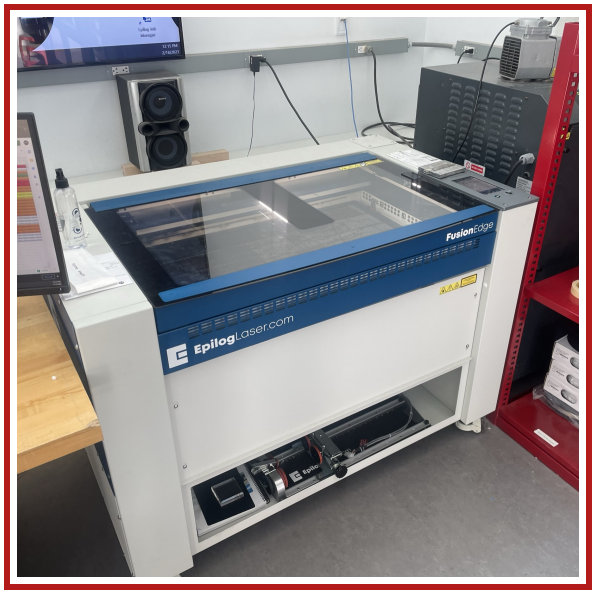

Figure 6.2.2: Cornell Rapid Prototyping Lab's Epilog Laser FusionEdge

6.3 Subsystem Manufacturing

6.3.1 Fuselage Manufacturing

The ribs, baseplate, and hatch of the fuselage are laser cut using the Cornell Rapid Prototyping Lab. Notches in the baseplate are used to align the ribs in the straight section into their correct locations. The carbon fiber spar slots in through these ribs and marked in order to provide the correct spacing for the ribs in the tapered section. Hardwood components are connected using standard wood glue, while cyanoacrylate is used between balsa components. Balsa stringers are made using a wooden strip cutter and trimmed to the correct length and glued in place. 3D printed integration pieces for the wing and tail attach through holes in the ribs and baseplate using screws and nuts. Velcro is attached surrounding the hatch using epoxy adhesive as other methods proved ineffective. After the structural assembly finished, MonoKote is applied surrounding the fuselage using irons and a heat gun in order to provide a streamlined finish.

6.3.2 Wing Manufacturing

The wing is composed primarily of wooden ribs, stringers, and spars which are all laser cut via Cornell's Rapid Prototyping Lab (RPL). The other main component, the carbon fiber spars, are cut to length with a band saw. The ribs are lined up on the carbon fiber spar and the servo plates were glued in between the ribs. The wooden spars and stringers are then glued to the ribs with cyanoacrylate. The ailerons were assembled similarly; they were lined up with a spar, the control horn plate was glued, and then stringers were glued to the ribs. The carbon fiber spars are then taken out and drilled with a drill press before being placed into the wings and glued. The Mission 3 adapters are then screwed and bolted into the carbon fiber spars. The servos are screwed and bolted into their plates. After all the pieces are installed, the wings and the ailerons are covered with MonoKote and heat shrunk separately. Ailerons are then connected to the wings via hinges that are glued into both pieces. The servo heads and control rods were then installed both with screws are then connected with steel control rods.

6.3.3 Empennage Manufacturing

The ribs, leading edge stringers, combs, and servo plates are laser cut using the RPL's laser cutting machine. The ribs of the horizontal stabilizer and elevators are first lined up to the combs and leading edge stringer before being glued together. The remaining stringers are glued with cyanoacrylate. The servo plate is wood glued between two ribs in the horizontal stabilizer and a corresponding hardwood plate is glued in the elevator to line up. The two elevators are connected using two dowel rods, ensuring they are fixed at the same angle of attack. The vertical stabilizer and rudder are assembled in a similar fashion with the addition of gluing in the two wooden dowel rods near the leading edge of the vertical stabilizer for structural stability. The horizontal tail is then wood glued into the baseplate and the vertical tail is attached to the assembly using a T-plate and the lower dowel rods. The servos for the elevator and rudder are installed in the horizontal and vertical stabilizers. Both stabilizers, the elevators, and the rudder are then all applied with MonoKote. The control surfaces are attached to the main tail using hinge points that are wood glued into combs in the trailing edges of the stabilizers and leading edges of the control surfaces. Control horns are then screwed into hardwood plates within the control surfaces. Steel control rods are installed to connect the servos and control horns using EZ Connectors.

6.3.4 Mission 2 Manufacturing

Due to the nature of the Mission 2 payload, only a few viable options were available for manufacturing this component. The decision was made early on to use a 3D printer since it would be difficult to replicate the box to the precision a machine can. After this, the decision on materials was limited due to what could work with the printers. After testing Onyx and resin, resin was found to be the strongest and most structurally stable for the mission due to its density and full infill.

The box and domino-style lid are both manufactured using the FormLabs 3+ resin 3D printer at the Cornell Rapid Prototyping Lab. Notches on the bottom of the box are used to align the box with the correct ribs and position in the fuselage, accessed through a built-in side door on the plane. The lid of the box is designed so that it would be able to be slide into a pre-built opening and still cover the entire top of the box. Cylindrical holes are designed as cut-outs on the inside of the box (which is otherwise filled with hard resin), to act as a location to put as-needed weights for the mission and to remove unnecessary weight caused by the full resin infill. For these, a cylindrical design and dimensions are chosen due to the original choice of test weights. The walls, notch, and lid of the payload are built to be thicker so as to allow for greater structural integrity and to better withstand future flights. Testing of older iterations was accomplished using both ABS and resin materials, with slightly different designs on each.

6.3.5 Mission 3 Manufacturing

Because of the forces that the integration piece must undergo and the complex geometry, the only viable option for manufacturing this part is 3D printing it. The 3D printer had many advantages: it is more precise and easy to make the integration piece in different materials to test them. It was decided to use Cornell's Rapid Prototyping Lab's FormLabs 3+ resin 3D printer. Because the integration piece is one body and quite small, it

is easy to quickly manufacture multiple of them. By design, the team ensured that the thicknesses of the parts were adequate to ensure no breakage would occur during flight. It is also easy to manufacture configurations for both wings because they are simply mirrored.

6.3.6 Ground Mission Manufacturing

The ground mission integration piece is 3D printed to ensure accuracy and fit with the mission three integration piece. The rest of the structure is composed of $1/4$" plywood that is laser cut and slotted, then assembled using L-brackets, screws, and attached with wood glue. Because of the probability of wood buckling, a 3.5-foot PVC pipe is slotted through the integration piece and supports the plane.

7 Testing Plan

7.1 Subsystem Tests

7.1.1 Static Thrust Test

Static thrust testing serves two purposes: to verify the values derived from eCalc simulations and to ensure that sufficient thrust was available for ten minutes of stable flight. Additionally, a wattmeter measured the current draw. This is used to estimate the amount of flight time for a fully charged battery on different throttle levels. When the propulsion combination in section 5.1.9 was selected, a static thrust test rig (Figure 7.1.1) was assembled using the same components. Tests at 100% power for take-off and at 60% power for the cruise were performed.

The propeller and motor are mounted on a rotating L-bar of equal length, with the other end placed on top of an electronic scale. As the motor spins, the propeller applies a thrust force on the L-bar, generating a moment about the pivot point. This moment is counteracted by the normal force by the electronic scale, which reads out the normal force being supplied. Since the L-bar is of equal length, the scale reading is equal to the amount of thrust being generated.

7.1.2 Wing Integration ANSYS Simulation

As the wing integration piece takes up all of the load during the ground mission and in flight, it is imperative that this structure is structurally durable and robust. ANSYS Workbench was used to verify the structural integrity of the wing integration piece. This analysis was performed by transferring a simplified Solidworks assembly of the wing integration piece and wing spars into ANSYS Workbench and assigning the correct material values to each component. A Young modulus of 2.4 GPa and yield strength of 40 MPa were assigned for Onyx filament as per the Markforged website. A Young's modulus of 228 GPa and Yield Strength of 4.4 GPa was assigned for the braided carbon fiber spars. With the end of the wing spars acting as the fixed support a 200N force was applied downwards to the fuselage spar. Figure 7.1.2 provides graphical results of the simulations.

The simulation resulted in a maximum Von-Mises stress of 15.5 MPa, and a maximum deformation of 0.3mm for the wing integration piece. Given the yield strength of Onyx as 40 MPa, this provides results for a factor of safety of 2.6. This factor of safety is large enough to account for unanticipated aircraft maneuvering

(a) (b)

Figure 7.1.1: Propulsion static thrust test rig. 7.1.1a and 7.1.1b give the top and side vies respectively

and loading during flight and will be able to sustain significant loads during ground testing. Moving forward, mechanical testing will be performed to confirm the simulation results and finalize target weight for competition.

7.2 Flight Testing Plan

Flight tests serve as valuable feedback towards the team as it validates expected performance parameters set out through simulations. Points of improvement for future iterations are noted, and the team undergoes a full revision process of the design before beginning a new iteration. Thus, it is vital that deadlines are met and that dates with favorable weather conditions are picked for flight test.

Toward the end of January, the team was able to perform its first flight test of its first iteration aircraft. This test was conducted mainly to increase familiarity with the aircraft's handling, ensure that all subsystems meshed together properly, and that stable flight could be generated. Due to setbacks in the manufacturing phase, this occurred later than the team had hoped (Iteration one of the aircraft was expected to be ready for a test flight before Cornell University's winter break). Nonetheless, the results of the test, detailed in Section 8.2, returned promising signs of a high-scoring and performing aircraft. The team fully expects to complete the fabrication of the second iteration in the coming weeks and continue flight testing to further validate the performance of the aircraft, including competition and mission simulations.

7.3 Flight Test Checklist

The following flight test checklist is used by the team to ensure the safety and preparedness for flight tests.

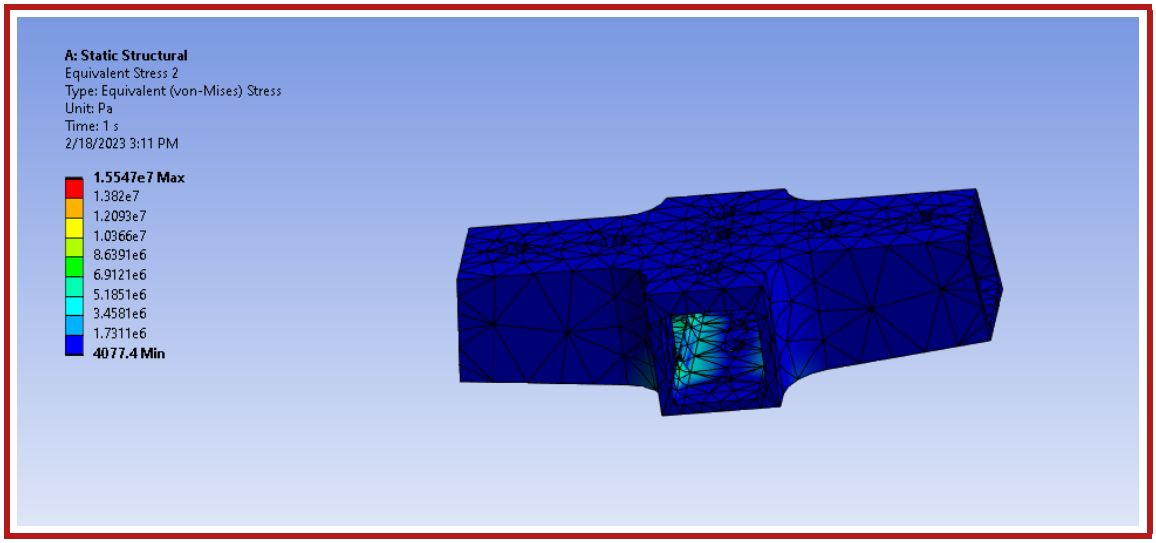

(a) Von-Mises stress analysis. A maximum stress of 2.25 ksi (15.5 MPa) occurs in the intersection of the spars.

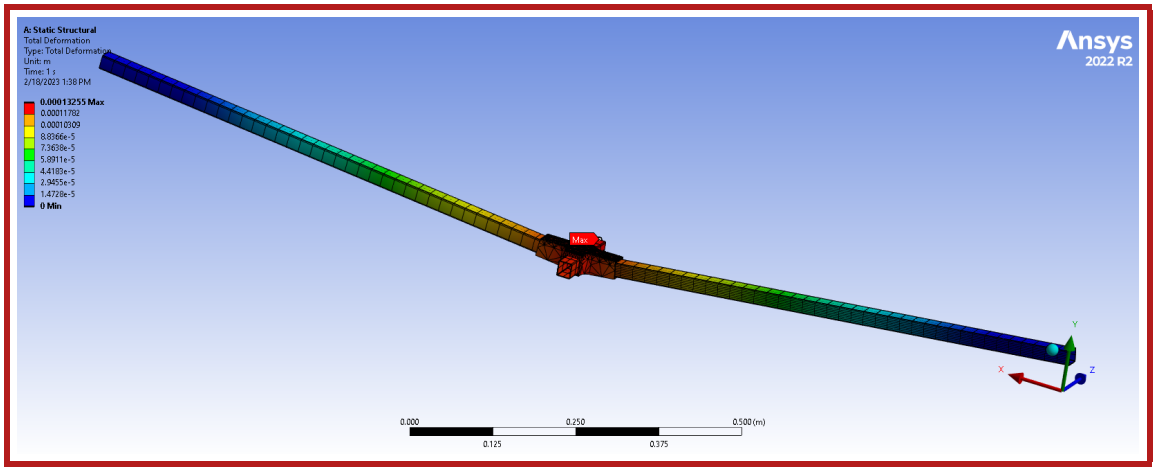

(b) Deflection analysis. A maximum deflection of $5.11e-3$ inches (0.13mm) occurs in the integration piece.

Figure 7.1.2: ANSYS Workbench Ground Test Simulation Results

Pre-Flight Checklist

Last Updated: 12/6/2021

Flight Test Date:_____

Task	✓	Remarks
Electrical Power Sources		
Verify Main Propulsion Battery at full charge		
Verify Receiver Battery at full charge		
Verify Transmitter Battery at full charge		
Aeronautics		
Verify wings are well secured to the fuselage		
Identify location of center of gravity		
Wingtip test		
Actuation		
Zero servos		
Correct servo connections to receiver, battery and ESC		
Ensure servos are securely fastened		
Verify control surfaces have enough deflection		
Propulsion		
Ensure correct propeller is mounted		
Ensure propeller is securely fastened		
Ensure we are using a Right (not Left) propeller		
Miscellaneous Tests		
Landing Gear/Roll Test		
Propulsion Mount Structural Test		
Transmitter Range Test		
Record total prop weight and total plane weight		
Flight Contingency Case Manifest		
LiPo Protective Bag	Y	
Electrical Tape, Duct Tape, Hinge Tape	Y	
Scissors, Xacto Knives (2)	Y	
Hand Drill and Drill Bits	Y	
CA Glue (2, Instant and Gap Filling) and Extra Tips	Y	
Balsa sheet (⅛, 1/16), balsa stringers	Y	
Extra Transmitter, Receiver, ESC	Y	
Thermal Blanket for Cold Weather		
2x sets of Allen Keys	Y	
Bolts and Nuts	Y	
Logistics		
Ensure weather conditions favorable		
File for FAA approval		

Pre-Takeoff Checklist

Task	✓	Remarks
50% Throttle, Throttle Closed, Full Up Elevator, Full Right Rudder, Full Right Aileron		
Radio Failsafe set, Arming plug in possession		
Propeller rotating in correct direction		
Favorable Wind, Weather Conditions		

Figure 7.3.1: CU DBF flight test checklist

8 Testing Results

8.1 Subsystem Test Results

8.1.1 Static Thrust Test Results

As described in Section 7.1.1, static thrust tests were conducted to verify values derived in eCalc and to ensure that sufficient thrust was available for ten minutes of stable flight. Each motor is connected to an Admiral 4500mAh 22.2V 80C Battery, Cobra 60A ESC, 30A fuse, watt meter, and arming switch all in series. Table 8.1.1 shows the results of the test.

Motor	Propeller Diameter (in)	Propeller Pitch (in)	Power Setting	Measured Static Thrust (lbs)	Predicted Static Thrust (lbs)	Current Drawn (A)
Cobra 4120-22 (430kV)	12	7	100% (Takeoff)	5.71	5.95	-
			60% (Cruise)	3.43	3.57	24

Table 8.1.1: Static Thrust Test Results

The flight time can be calculated by taking the battery's capacity in amp hours, then dividing that into the average amp drawn of the motor ($(4.5Ah/24A) \times 60$ minutes $= 11.3$ minutes)

This shows that the plane is capable of flying for 11.3 minutes. Given that the plane needs to fly for 10 minutes during Mission 1, the extra capacity can be accounted for landing as the landing time is not accounted in the 10 minutes.

To verify the aircraft's endurance, the propulsion subteam also ran an endurance test with the selected propulsion system on the static thrust testing rig. Setting the power at cruise speed, the propulsion system was able to sustain more than 15 minutes of cruise power before the team decided to end the test. This further validates the aircraft's performance and results, and gives the team confidence that the aircraft can sustain flight for the entirety of Mission two and other flight missions.

The measured static thrust is slightly lower than the predicted thrust from eCalc. The measured thrust of 5.71 lbs is around 97% of what was expected. There are many variables that could have led to this, including battery performance being affected by cold weather or not fully charged, uncertainty of the electronic scale etc.

8.2 Flight Test Results

Over the course of January and February, the team was able to conduct a few flight tests during to keep track of overall progress, assess qualitatively how the aircraft was performing at different stages of development, and provide feedback and suggestions for improvement. Notably, key systems requirements were checked to ensure that the aircraft conformed to the DBF rule set and met our requirements set out.

For the first iteration of the aircraft, the team was able to successfully take off within the stipulated 60 feet of runway (SYS 4). The aircraft was able to climb out and turn successfully to the right and sustain about five seconds of stable flight before a hard bank angle was initiated (unclear if due to pilot error or roll instability)

and the aircraft lost lift, causing the aircraft to stall and crash. Unfortunately, the crash led to a complete loss of the fuselage body, but the team was fortunately able to recover the wing, tail, and propulsion system with minimal damage. Mission 2 and Mission 3 systems were not fully tested in this iteration, although successful flight validated the propulsion system and aerodynamics design, and the team has full confidence that the aircraft will improve in future iterations and flight tests.

(a) BR-23 Vermillion on before takeoff roll

(b) BR-23 Vermillion in flight

Figure 8.2.1: Test flight photos of iteration 1 of BR-23 Vermillion

References

[1] *AIAA DBF Rules 2023*. AIAA Foundation. Sept. 2022.

[2] MATLAB. *version 9.13.0 (R2022b)*. Natick, Massachusetts: The MathWorks Inc., 2022.

[3] Tjoetjoek Eko Pambagjo, Kazuhiro Nakahashi, and Kisa Matsushima. "Flying Wing Concept for Medium Size Airplane". In: *ICAS 2002: 23rd International Congress of Aeronautical Sciences, Proceedings, Toronto, Canada, 8 to 13 September, 2002*. International Council of the Aeronautical Sciences(ICAS), 2002, pp. 153.1–153.8.

[4] Roelof Vos. "Flying V: An Efficient Airfram for Long-Haul Transport". In: *Innovation For A Green Transition: 2022 Environmental Report*. International Civial Aviation Organization, 2022, pp. 116–119.

[5] Snorri Gudmundsson. *General Aviation Aircraft Design*. Elsevier, Inc, 2014.

[6] Daniel P. Raymer. *Aircraft design: A conceptual approach*. American Institute of Aeronautics and Astronautics, 2021.

[7] Markus Mueller. *PROPCALC - the most reliable propeller calculator on the web*. Apr. 2017. URL: https://www.ecalc.ch/motorcalc.php.

[8] Jack Lambie. *Designing and Building Composite R/C Model Aircraft*. Motorbooks International, 1987.

[9] Kenn Meyers. *Wing cube loading (WCL)*. May 2018. URL: https://www.sefsd.org/general-interest/wing-cube-loading-wcl/.

[10] Andrew Wood. *Aircraft Horizontal and Vertical Tail Design*. Sept. 2022. URL: https://aerotoolbox.com/design-aircraft-tail/.

[11] *Markforged Onyx Data Sheet*. Oct. 2022. URL: https://support.markforged.com/portal/s/article/Onyx.